



ELSEVIER

Contents lists available at ScienceDirect

Journal of the Mechanics and Physics of Solids

journal homepage: www.elsevier.com/locate/jmps

Cavitation in elastomeric solids: I—A defect-growth theory

Oscar Lopez-Pamies^{a,*}, Martín I. Idiart^{b,c}, Toshio Nakamura^a^a Department of Mechanical Engineering, State University of New York, Stony Brook, NY 11794-2300, USA^b Departamento de Aeronáutica, Facultad de Ingeniería, Universidad Nacional de La Plata, Calles 1 y 47, La Plata B1900TAG, Argentina^c Consejo Nacional de Investigaciones Científicas y Técnicas (CONICET), Avda. Rivadavia 1917, Cdad. de Buenos Aires C1033AAJ, Argentina

ARTICLE INFO

Article history:

Received 3 November 2010

Received in revised form

15 April 2011

Accepted 16 April 2011

Keywords:

Finite strain

Microstructures

Homogenization methods

Instabilities

Bifurcation

ABSTRACT

It is by now well established that loading conditions with sufficiently large triaxialities can induce the sudden appearance of internal cavities within elastomeric (and other soft) solids. The occurrence of such instabilities, commonly referred to as cavitation, can be attributed to the growth of pre-existing defects into finite sizes. This paper introduces a new theory to study the phenomenon of cavitation in soft solids that: (i) allows to consider general 3D loading conditions with arbitrary triaxiality, (ii) applies to large (including compressible and anisotropic) classes of nonlinear elastic solids, and (iii) incorporates direct information on the initial shape, spatial distribution, and mechanical properties of the underlying defects at which cavitation can initiate. The basic idea is to first cast cavitation in elastomeric solids as a homogenization problem of nonlinear elastic materials containing random distributions of zero-volume cavities, or *defects*. This problem is then addressed by means of a novel iterated homogenization procedure, which allows to construct solutions for a specific, yet fairly general, class of defects. These include solutions for the change in size of the defects as a function of the applied loading conditions, from which the onset of cavitation — corresponding to the event when the initially infinitesimal defects suddenly grown into finite sizes — can be readily determined. In spite of the generality of the proposed approach, the relevant calculations amount to solving tractable Hamilton–Jacobi equations, in which the initial size of the defects plays the role of “time” and the applied load plays the role of “space”. When specialized to the case of hydrostatic loading conditions, isotropic solids, and defects that are vacuous and isotropically distributed, the proposed theory recovers the classical result of Ball (1982) for radially symmetric cavitation. The nature and implications of this remarkable connection are discussed in detail.

© 2011 Elsevier Ltd. All rights reserved.

1. Introduction

Experimental evidence (Gent and Lindley, 1959; Gent and Park, 1984; Dorfmann, 2003; Bayraktar et al., 2008; Cristiano et al., 2010) has shown that loading conditions with sufficiently large triaxialities can induce the sudden appearance of internal cavities in elastomers and other soft solids. The occurrence of such instabilities, commonly referred to as cavitation, has been attributed to the growth of pre-existing defects (Gent, 1991). In a typical elastomer, defects are expected to appear randomly distributed and to have a wide range of sizes with average diameters fluctuating

* Corresponding author. Tel.: +1 6316328249; fax: +1 6316328544.

E-mail addresses: oscar.lopez-pamies@sunysb.edu (O. Lopez-Pamies), martin.idiart@ing.unlp.edu.ar (M.I. Idiart), toshio.nakamura@sunysb.edu (T. Nakamura).

around 0.1 μm . But beyond these geometrical features not much is known about their nature — they may possibly correspond to actual holes, particles of dust, and/or even weak regions of the polymer network (Gent, 1991).

From a practical point of view, the occurrence of cavitation is an important phenomenon because it may signal the initiation of material failure, since upon continuing loading a number of “nucleated cavities” may grow, coalesce, and eventually form large enclosed cracks (Gent and Lindley, 1959). This is particularly important in the contexts of reinforced elastomers (Gent and Park, 1984; Cho et al., 1987; Michel et al., 2010) and structures bonded together with soft adhesives (Creton and Hooker, 2001), where the regions surrounding the inherent soft/stiff interfaces are prone to develop high stress triaxialities. Alternatively, the phenomenon of cavitation can be used to an advantage. A prominent example is that of rubber-toughened hard brittle polymers, where the cavitation and post-cavitation behavior of the rubber particles provides an essential toughening mechanism (Cheng et al., 1995; Steenbrink and Van der Giessen, 1999). More recently, cavitation has also been proposed as a means to indirectly measure the mechanical properties of soft materials (Kundu and Crosby, 2009).

In a pioneering effort to analyze cavitation in elastomeric solids, Gent and Lindley (1959) examined the nonlinear elastostatics problem of a single vacuous spherical cavity of finite size embedded in an infinite matrix subjected to uniform hydrostatic pressure on its boundary (i.e., at infinity). Assuming the matrix to be an incompressible Neo-Hookean solid, they found that as the applied pressure approaches the critical value $P_{cr} = 5\mu/2$ (with μ denoting the shear modulus of the matrix material in the ground state) the size of the cavity becomes unbounded, and therefore cavitation ensues. Remarkably, this predicted value turned out to be in good agreement with some of their experimental measurements on vulcanized natural rubber. In a different approach, Ball (1982) later considered cavitation not as the growth of defects but rather as a class of non-smooth bifurcations. Specifically, he analyzed the problem of a unit ball (in n dimensions), made out of isotropic nonlinear elastic material, that is subjected to hydrostatic loading on its boundary. By means of a variety of techniques from the theory of ordinary differential equations and the calculus of variations, he showed that when the applied load is small the ball remains a solid ball, but that when the load is sufficiently large it may be energetically more favorable for the material to open up a spherical (or, if $n=2$, circular) cavity at the center of the ball. For well understood reasons (Ball, 1982; Sivaloganathan, 1986; Sivaloganathan et al., 2006), the above two approaches lead to identical critical applied pressures at which cavitation ensues in *isotropic* solids subjected to *hydrostatic* loading. This suggests that the phenomenon of cavitation in nonlinear elastic solids can be viewed rather equivalently as: (i) the sudden growth of pre-existing defects or (ii) a non-smooth bifurcation in an initially defect-free material. In this work, as detailed in Section 2, we will consider the phenomenon of cavitation as the growth of pre-existing defects.

The prime results of Gent and Lindley (1959) and of Ball (1982) are based on the conditions that:

- The applied loading is *hydrostatic*.
- The material behavior is *incompressible* and *isotropic*.
- In the case of Gent and Lindley, the pre-existing defect is assumed to be a *single vacuous spherical cavity*, while in the analogous result of Ball, the formation of a *single vacuous spherical cavity* is the only bifurcation allowed in the analysis.

Over the last three decades, numerous efforts have been devoted to extend the above results to more general loading conditions, material behaviors, and types of defects/bifurcations. In the next three paragraphs, we recall the underlying physical motivation to carry out such generalizations and outline the major findings of hitherto efforts together with key remaining open problems, which we aim to tackle in this paper.

The occurrence of cavitation is expected (Gent and Tompkins, 1969a; Chang et al., 1993; Bayraktar et al., 2008) to depend intricately on the entire state of the applied loading conditions and not just on the hydrostatic component. Yet, the vast majority of cavitation studies to date have been almost exclusively limited to the case of hydrostatic loading conditions, presumably because of its simpler tractability. Among the exceptions, Hou and Abeyaratne (1992) have made use of variational arguments to derive an approximation for the onset of cavitation in incompressible isotropic solids subjected to loadings with arbitrary triaxiality. Sivaloganathan, Spector, and co-workers (Sivaloganathan and Spector, 2000, 2002; Sivaloganathan et al., 2006; see also Henao, 2009) have established, via energy-minimization techniques, existence results for the onset of cavitation in isotropic polyconvex solids under fairly general loadings. More recently, Lopez-Pamies (2009) has derived a variational approximation for the onset of cavitation in isotropic materials subjected to loadings with arbitrary 2D triaxiality by means of a “linear comparison” homogenization technique (Lopez-Pamies and Ponte Castañeda, 2006).

Elastomers are of course *not* exactly incompressible but in actuality they exhibit finite bulk moduli that can range from as much as 4 (nearly incompressible) to as little as 1 (very compressible) orders of magnitude larger than their shear moduli, depending on how they are synthesized/fabricated (Bridgman, 1945; Arridge and Folkes, 1972; Bischoff et al., 2001). In an attempt to accommodate this material compressibility, extensions of the works of Gent and Lindley and of Ball have been proposed, although in the restricted context of hydrostatic loading conditions (Stuart, 1985; Sivaloganathan, 1986; Horgan and Abeyaratne, 1986). Moreover, depending on their processes of synthesis/fabrication, elastomers can also exhibit sizable degrees of anisotropy (Sohoni and Mark, 1987; Warner and Terentjev, 2005). However, with the exception of a few idealized studies (Antman and Negrón-Marrero, 1987; Merodio and Saccomandi, 2006), very little progress has been made thus far in the analysis of cavitation in anisotropic materials, especially those with physically relevant anisotropies (e.g., transverse isotropy, orthotropy).

In addition to the loading conditions and type of material behavior, it is expected that the initial shape and spatial distribution of pre-existing defects are geometrical features that may impact when and how cavitation occurs. Yet, existing cavitation studies have primarily focused on material systems containing a single defect of spherical (or circular) shape (Horgan and Polignone, 1995; Fond, 2001). It is only recent that studies on single cavities of non-spherical shape (James and Spector, 1991) and on large number of point defects at which cavitation can initiate (Sivaloganathan and Spector, 2000, 2002; Sivaloganathan et al., 2006; Henao, 2009) have begun to be pursued. Besides geometrical attributes, defects possess mechanical properties as well, although very little is known about them. The simplest hypothesis is to consider that they are vacuous (i.e., traction-free cavities), as was assumed in the original works of Gent and Lindley (1959) and of Ball (1982), and in most subsequent efforts (Horgan and Polignone, 1995; Fond, 2001). Under suitable circumstances, however, it is known that defects may contain a non-zero pressure (Gent and Tompkins, 1969a; Sivaloganathan, 1999). How pressurized defects, and, more generally, defects with more non-trivial mechanical properties, impact cavitation remains to be thoroughly examined.

In this paper, we propose a new strategy to study cavitation in elastomeric solids that is general enough to address the open problems spelled out in the preceding paragraphs¹ and, at the same time, is also simple enough to lead to tractable solutions. More specifically, the proposed approach allows to construct onset-of-cavitation criteria that (i) are valid for general 3D loading conditions with arbitrary triaxiality and (ii) large (including compressible and anisotropic) classes of nonlinear elastic solids, (iii) incorporate direct information on the initial shape, spatial distribution, and mechanical properties of the underlying defects at which cavitation can initiate, and, in spite of accounting for this refined information, (iv) are analytically tractable. The strategy consists essentially of two steps:

- First, motivated by the recent work of Lopez-Pamies (2009), we begin by casting the phenomenon of cavitation as the homogenization problem of nonlinear elastic materials containing random distributions of disconnected zero-volume cavities, or *defects*. The key advantage of this approach over earlier perspectives is that it compactly reduces the analysis of cavitation to the computation of two *average* quantities: the total elastic energy of the solid containing the cavities and the associated current volume fraction of cavities in affinely deformed states. This idea is shown schematically in Fig. 1. The onset of cavitation along a given loading path corresponds simply to the event when the initially infinitesimal volume fraction of cavities suddenly grows into finite values.
- Second, by means of an innovative iterated homogenization procedure, we construct exact solutions for a particular class of random distributions of cavities, which ultimately lead to a fairly general and explicit framework to derive onset-of-cavitation criteria. In spite of its generality, the analysis of the proposed formulation reduces to the study of two Hamilton–Jacobi equations, one for the total elastic energy and one for the current volume fraction of cavities, in which the initial infinitesimal volume fraction of the cavities plays the role of “time” and the applied load plays the role of “space”.

The paper is organized as follows. In Section 2, we set up the problem of cavitation in elastomeric solids as a homogenization problem in nonlinear elasticity and give a formal definition of onset of cavitation in terms of homogenized quantities. The iterated homogenization method is presented in Section 3. The main result of this paper is given by the onset-of-cavitation criterion (48)–(50) in Section 4. Sections 4.1–4.3 discuss various physically motivated specializations of the proposed framework including those to incompressible and isotropic material systems, as well as to hydrostatic loading conditions. In Section 5, we recall the classical criterion of Ball (1982) for radially symmetric cavitation of isotropic materials and show that our formulation corresponds in actuality to a generalization of this classical result to loading conditions with arbitrary triaxiality, compressible anisotropic nonlinear elastic materials, and fairly general types of defects. Finally, Section 6 presents some concluding remarks.

2. Problem formulation: cavitation as the sudden growth of defects

The phenomenon of cavitation is taken here to correspond to the sudden growth of defects present in a solid in response to sufficiently large applied external loads, as schematically depicted in Fig. 1. Defects, in turn, are assumed to be nonlinear elastic cavities of zero volume, but of arbitrary shape otherwise, that are randomly distributed throughout the solid. In this section, these ideas are cast into a mathematical formulation, roughly speaking, by first considering the homogenization problem of a nonlinear elastic solid containing a *finite* initial volume fraction of disconnected cavities, and then evaluating the limit as this volume fraction tends to zero.

We begin by considering a material made up of a random distribution of disconnected cavities embedded in an otherwise homogeneous matrix phase. A specimen of such a material is assumed to occupy a volume Ω_0 , with boundary $\partial\Omega_0$, in the undeformed stress-free configuration. The cavities occupy a finite volume fraction $f_0 = |\Omega_0^{(2)}|/|\Omega_0|$ of the

¹ In addition to the considerations on loading conditions, material behavior, and the geometric and constitutive nature of defects, surface-energy, fracture, and dynamic effects could also play a role in the occurrence of cavitation in elastomeric solids (see, e.g., Gent and Tompkins, 1969b; Müller and Spector, 1995; Williams and Schapery, 1965; Henao and Mora-Corral, 2010; Pericak-Spector and Spector, 1988). These aspects, however, will not be considered in this work.

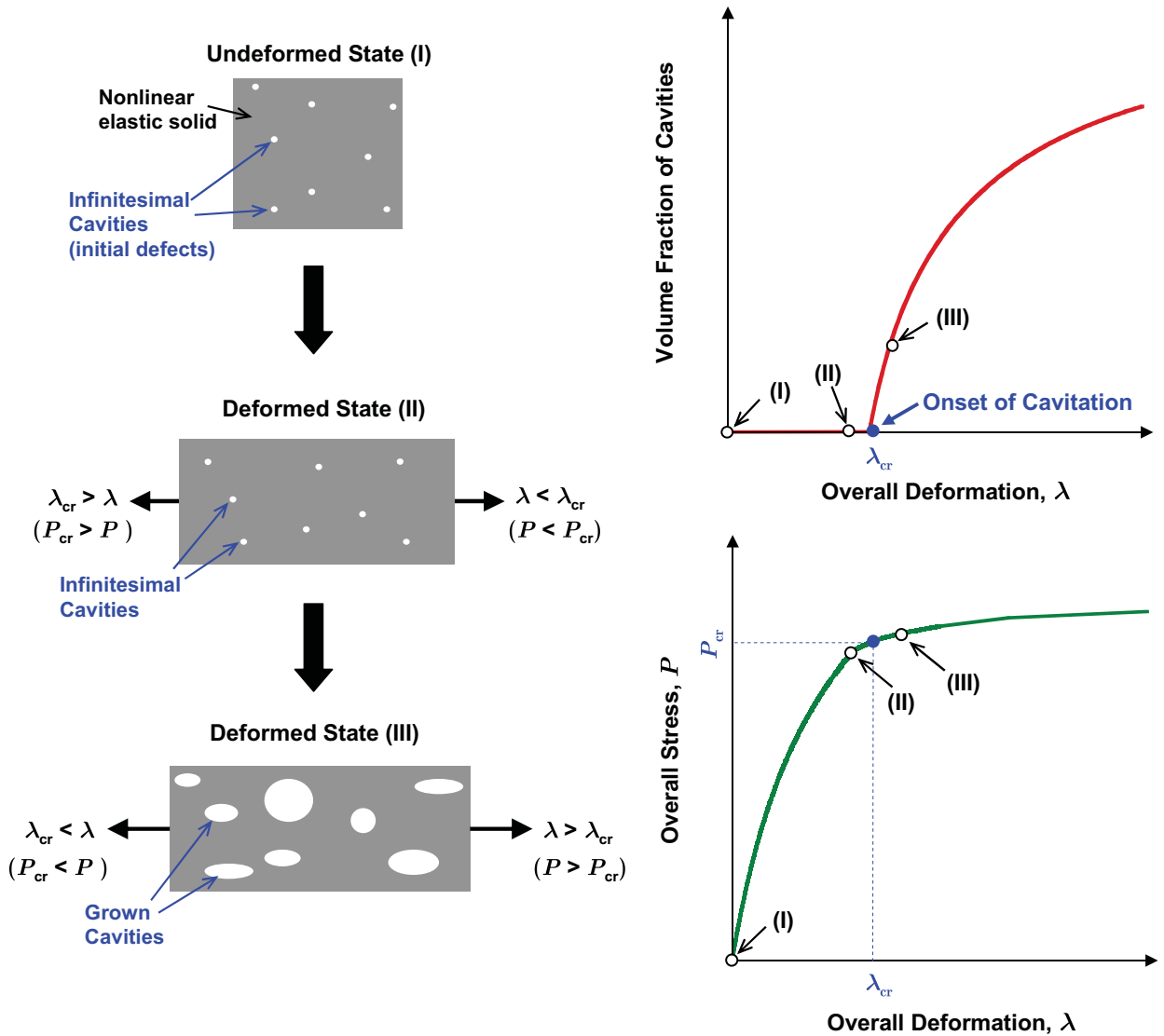


Fig. 1. Schematic illustrating the phenomenon of cavitation as the growth of pre-existing infinitesimally small cavities (or defects). In the undeformed state, the volume fraction of cavities is infinitesimal and remains infinitesimal along any given loading path up to a critical applied load, with overall deformation λ_{cr} and overall stress P_{cr} , at which it suddenly becomes of finite size. This event corresponds to the onset of cavitation. Upon further loading, beyond the onset of cavitation, the volume fraction of cavities increases and the overall stress severely softens, as a result of the continuing growth of the cavities into larger sizes.

undeformed configuration, but their characteristic length scale is considered to be much smaller than the size of Ω_0 . It is further assumed that the random distribution is statistically uniform and ergodic.

Material points in the solid are identified by their initial position vector \mathbf{X} in the undeformed configuration Ω_0 , while the current position vector of the same point in the deformed configuration Ω is given by $\mathbf{x} = \chi(\mathbf{X})$. Motivated by physical arguments, the mapping χ is required to be continuous (i.e., the material is not allowed to fracture) and one-to-one on Ω_0 (i.e., the material is not allowed to interpenetrate itself). In addition, we assume that χ is twice continuously differentiable, except possibly on the cavities/matrix boundaries. Note that this degree of regularity is not too restrictive for our purposes since the only “singularities” of interest (i.e., the cavities) are pre-existing ones. The deformation gradient \mathbf{F} at \mathbf{X} is defined by

$$\mathbf{F} = \text{Grad } \chi \quad \text{in } \Omega_0 \tag{1}$$

and satisfies the local material impenetrability constraint $J \equiv \det \mathbf{F} > 0$.

Both the matrix ($s=1$) and the cavities ($s=2$) are taken to be nonlinear elastic solids characterized by stored-energy functions $W^{(s)}$ of \mathbf{F} . These functions are assumed to be non-negative, continuously differentiable, objective, and

quasiconvex. The present analysis is thus general enough to allow for non-vacuous cavities² characterized by some non-zero stored-energy function $W^{(2)}$. No further requirements on $W^{(s)}$ are imposed at this point, except for the usual assumption that

$$W^{(s)}(\mathbf{F}) = \frac{1}{2}\boldsymbol{\varepsilon} \cdot \mathcal{L}^{(s)}\boldsymbol{\varepsilon} + O(\|\mathbf{F}-\mathbf{I}\|^3) \quad (2)$$

in the limit as $\mathbf{F} \rightarrow \mathbf{I}$ for consistency with the classical theory of linear elasticity. In the above expression, $\boldsymbol{\varepsilon} = (\mathbf{F} + \mathbf{F}^T - 2\mathbf{I})/2$ is the infinitesimal strain tensor, and $\mathcal{L}^{(s)} = \partial^2 W^{(s)}(\mathbf{I})/\partial \mathbf{F}^2$ are fourth-order modulus tensors. While we will restrict attention to matrix phases with positive definite modulus tensors $\mathcal{L}^{(1)}$, the modulus tensor $\mathcal{L}^{(2)}$ is only restricted to be positive semi-definite in order to allow for the possibility of vacuous cavities. At each material point \mathbf{X} in the undeformed configuration, the first Piola–Kirchhoff stress \mathbf{S} is related to the deformation gradient \mathbf{F} by

$$\mathbf{S} = \frac{\partial W}{\partial \mathbf{F}}(\mathbf{X}, \mathbf{F}), \quad W(\mathbf{X}, \mathbf{F}) = (1 - \theta_0(\mathbf{X}))W^{(1)}(\mathbf{F}) + \theta_0(\mathbf{X})W^{(2)}(\mathbf{F}), \quad (3)$$

where θ_0 is the characteristic function that takes the value 1 if the position vector \mathbf{X} is in a cavity, and 0 otherwise, and serves therefore to describe the microstructure (here, the size, shape, and spatial location of the cavities) in the undeformed configuration Ω_0 .

More specifically, the function θ_0 in (3) is a random variable that must be characterized in terms of ensemble averages (Willis, 1981, 1982). Thus, the ensemble average of $\theta_0(\mathbf{X})$ represents the one-point probability $p_0^{(2)}(\mathbf{X})$ of finding a cavity at \mathbf{X} ; the ensemble average of $\theta_0(\mathbf{X})\theta_0(\mathbf{X}')$ represents the two-point probability $p_0^{(22)}(\mathbf{X}, \mathbf{X}')$ of finding cavities simultaneously at \mathbf{X} and \mathbf{X}' . Higher order probabilities are defined similarly. In view of the assumed statistical uniformity and ergodicity, the one-point probability can be identified with the initial volume fraction of cavities (Willis, 1982)

$$p_0^{(2)}(\mathbf{X}) = \frac{|\Omega_0^{(2)}|}{|\Omega_0|} = f_0, \quad (4)$$

which measures the relative size of the cavities, while the two-point probability contains information about the shape and spatial distribution of the cavities, and can be written as

$$p_0^{(22)}(\mathbf{X}, \mathbf{X}') = f_0^2 + (1 - f_0)f_0 h(\mathbf{X} - \mathbf{X}') \quad (5)$$

for some even function h with $h(\mathbf{0}) = 1$. As will be discussed in more detail below, the theory to be developed in Section 3 will incorporate information up to two-point probabilities.

We suppose now that the body is subjected to the affine displacement boundary condition

$$\mathbf{x} = \bar{\mathbf{F}}\mathbf{X} \quad \text{on } \partial\Omega_0, \quad (6)$$

where the second-order tensor $\bar{\mathbf{F}}$ is a prescribed quantity; here, it should be emphasized that because of the assumed quasiconvexity of W , separation of length scales, and statistical uniformity there is no need (Hill, 1972) to consider more general boundary conditions than (6). In the absence of body forces, it follows that the total elastic energy (per unit undeformed volume) stored in the material is formally given by

$$E = \min_{\mathbf{F} \in \mathcal{K}(\bar{\mathbf{F}})} \frac{1}{|\Omega_0|} \int_{\Omega_0} W(\mathbf{X}, \mathbf{F}) \, d\mathbf{X}, \quad (7)$$

where \mathcal{K} stands for the set of kinematically admissible deformation gradient fields:

$$\mathcal{K}(\bar{\mathbf{F}}) = \{\mathbf{F} : \exists \boldsymbol{\chi} = \boldsymbol{\chi}(\mathbf{X}) \text{ with } \mathbf{F} = \text{Grad} \boldsymbol{\chi}, J > 0 \text{ in } \Omega_0, \mathbf{x} = \bar{\mathbf{F}}\mathbf{X} \text{ on } \partial\Omega_0\}. \quad (8)$$

The equilibrium equations,³ namely, the Euler–Lagrange equations associated with the variational problem (7), reduce to the form

$$\text{Div} \left[\frac{\partial W}{\partial \mathbf{F}}(\mathbf{X}, \mathbf{F}) \right] = \mathbf{0} \quad \text{in } \Omega_0. \quad (9)$$

For later use, we also record here that the average first Piola–Kirchhoff stress over the undeformed configuration Ω_0 can be expediently written⁴ in terms of the total elastic energy (7) as

$$\bar{\mathbf{S}} \doteq \frac{1}{|\Omega_0|} \int_{\Omega_0} \mathbf{S}(\mathbf{X}) \, d\mathbf{X} = \frac{\partial E}{\partial \bar{\mathbf{F}}}, \quad (10)$$

and that the Cauchy stress averaged over the deformed configuration Ω can in turn be expressed as

$$\bar{\mathbf{T}} \doteq \frac{1}{|\Omega|} \int_{\Omega} \mathbf{T}(\mathbf{x}) \, d\mathbf{x} = \bar{J}^{-1} \bar{\mathbf{S}} \bar{\mathbf{F}}^T, \quad (11)$$

where $\bar{J} \doteq \det \bar{\mathbf{F}}$.

² Such as pressurized cavities, for instance.

³ The rotational balance $\mathbf{S}\mathbf{F}^T = \mathbf{F}\mathbf{S}^T$ is automatically satisfied because of the assumed objectivity of the stored-energy functions $W^{(1)}$ and $W^{(2)}$.

⁴ Identities (10) and (11) are direct consequences of the divergence theorem.

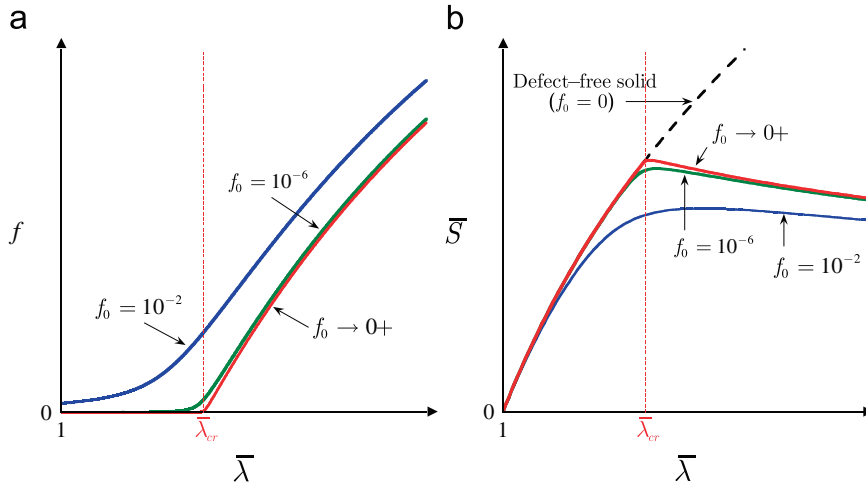


Fig. 2. One-dimensional schematic illustrating typical results for (a) the current volume fraction of cavities f and (b) the average stress $\bar{S} = dE/d\bar{\lambda}$ for various values of small initial volume fractions of cavities f_0 , as functions of the applied deformation $\bar{\lambda}$. In the limit as $f_0 \rightarrow 0+$, f is infinitesimal in the undeformed configuration ($\bar{\lambda} = 1$) and remains infinitesimally small for large applied deformations ($\bar{\lambda} > 1$) until a critical deformation $\bar{\lambda}_{cr}$ is reached at which it abruptly becomes finite and therefore cavitation ensues. At that same critical deformation, the overall stress \bar{S} reaches a critical value after which it severely softens, as a result of the growth of the cavities into finite sizes.

Of primary importance for studying cavitation is the growth of cavities upon deformation of the solid. Within the present formulation, an appropriate measure of cavity growth is given by the volume fraction of cavities in the *deformed* configuration. This quantity can be written as

$$f = \frac{|\Omega^{(2)}|}{|\Omega|} = \frac{f_0}{\bar{J}} \frac{1}{|\Omega_0^{(2)}|} \int_{\Omega_0^{(2)}} \det \mathbf{F}(\mathbf{X}) \, d\mathbf{X}, \quad (12)$$

where $\Omega^{(2)}$ is the domain occupied by the cavities in the deformed configuration, $\mathbf{F}(\mathbf{X})$ is the minimizing field in (7), and use has been made of the fact that $\det \mathbf{F}(\mathbf{X})$ is a null Lagrangian.

In the limit as $f_0 \rightarrow 0+$, the material under consideration in the above elastostatics problem reduces to a nonlinear elastic solid with stored-energy function $W^{(1)}$ containing a random distribution of (zero-volume cavities or) *defects* with stored-energy function $W^{(2)}$ and prescribed multi-point probabilities describing their shape and spatial location. When the material is finitely deformed according to (6), the size of these defects (as measured by their volume fraction f in the deformed configuration) can suddenly grow to finite values, signaling the onset of cavitation. To illustrate this event, Fig. 2 shows the one-dimensional schematic of a typical cavitating solution to the above elastostatics problem. Plots are given of the current volume fraction of cavities f and the average stress $\bar{S} = dE/d\bar{\lambda}$ versus an applied loading parameter $\bar{\lambda} \geq 1$ ($\bar{\lambda} = 1$ in the undeformed configuration) for decreasing values of f_0 . From part (a) of the figure, it is observed that f remains fairly constant up to some threshold in applied loading, after which it grows very rapidly. This sudden growth becomes increasingly sharper with decreasing values of initial volume fraction of cavities f_0 . In the limit as $f_0 \rightarrow 0+$, f tends to zero within the interval $1 \leq \bar{\lambda} \leq \bar{\lambda}_{cr}$ with $\bar{\lambda}_{cr}$ denoting the critical applied load at which the volume fraction of cavities suddenly becomes finite and therefore at which cavitation ensues. This sudden growth of f is accompanied by a pronounced softening in the overall stress response of the material, as shown in part (b) of the figure.

The occurrence of cavitation in nonlinear elastic solids can thus be expediently examined from the asymptotic behaviors of the total elastic energy (7) and current volume fraction of cavities (12) in the limit as $f_0 \rightarrow 0+$. To put this observation in a more rigorous setting, we introduce the functions

$$f_*(\bar{\mathbf{F}}) \doteq \lim_{f_0 \rightarrow 0+} f(\bar{\mathbf{F}}; f_0) \quad \text{and} \quad \bar{\mathbf{S}}_*(\bar{\mathbf{F}}) \doteq \lim_{f_0 \rightarrow 0+} \frac{\partial E}{\partial \bar{\mathbf{F}}}(\bar{\mathbf{F}}; f_0), \quad (13)$$

and postulate:

The onset of cavitation in a nonlinear elastic material with stored-energy function $W^{(1)}$ containing a random distribution of defects with stored-energy function $W^{(2)}$ occurs at critical deformations $\bar{\mathbf{F}}_{cr}$ such that

$$\bar{\mathbf{F}}_{cr} \in \partial \mathcal{Z}[f_*(\bar{\mathbf{F}})] \quad \text{and} \quad 0 < \|\bar{\mathbf{S}}_*(\bar{\mathbf{F}}_{cr})\| < +\infty, \quad (14)$$

where $\partial \mathcal{Z}[f_*(\bar{\mathbf{F}})]$ denotes the boundary of the zero set of the function $f_*(\bar{\mathbf{F}})$. The corresponding first Piola–Kirchhoff and Cauchy critical stresses at cavitation are given respectively by

$$\bar{\mathbf{S}}_{cr} = \bar{\mathbf{S}}_*(\bar{\mathbf{F}}_{cr}) \quad \text{and} \quad \bar{\mathbf{T}}_{cr} = \bar{J}_{cr}^{-1} \bar{\mathbf{S}}_{cr} \bar{\mathbf{F}}_{cr}^T, \quad (15)$$

where $\bar{J}_{cr} = \det \bar{\mathbf{F}}_{cr}$.

The graph of $f, (\bar{\mathbf{F}})$ in condition (14)₁ is a multidimensional version of the curve for $f_0 \rightarrow 0+$ in Fig. 2(a). The condition (14)₂, where the notation $\|\cdot\|$ indicates the Euclidean norm of a tensor, rules out deformation states associated with stress-free configurations and with unbounded stresses, at which cavitation cannot physically occur. Furthermore, we remark that the set of all critical deformations $\bar{\mathbf{F}}_{cr}$ satisfying the above criterion defines an onset-of-cavitation surface in deformation space, while the sets of all critical stresses $\bar{\mathbf{S}}_{cr}$ and $\bar{\mathbf{T}}_{cr}$ define onset-of-cavitation surfaces on first Piola–Kirchhoff and Cauchy stress spaces, respectively.

At this stage, it is important to recognize that the elastostatics problem (7) corresponds to nothing more than to the *homogenization problem* of a nonlinear elastic solid weakened by a random distribution of disconnected cavities (see, e.g., Müller, 1987; Lopez-Pamies and Ponte Castañeda, 2007; Michel et al., 2007; deBotton and Shmuel, 2010); in homogenization parlance, the quantity E given by (7) is commonly referred to as the macroscopic or effective stored-energy function, a terminology that will be used at various stages in the sequel. The key advantage of formulating the problem of cavitation as proposed above should now be apparent: expressions (7) and (12) are *homogenized* or *global quantities* (in particular, they are volume average quantities), and hence they are expected to be much easier to handle than *local fields*, such as for instance the deformation gradient $\mathbf{F}(\mathbf{X})$ itself, which would likely contain an excess of detail and thus would complicate unnecessarily the analysis of cavitation. At any rate, the computation of (7) and (12) is, in general, an extremely difficult endeavor because of the non-convexity of $W^{(1)}$ and $W^{(2)}$, and the randomness of the distribution of cavities, as characterized by θ_0 . In the next section, however, we propose a new method that will allow us to generate *exact solutions* for E and f for large families of material behaviors $W^{(1)}$ and $W^{(2)}$ and fairly general classes of random distributions of cavities θ_0 .

Finally, we remark that because of the non-convexity of W in \mathbf{F} , the solution to the Euler–Lagrange equation (9) need *not* be unique. However, given the asymptotic quadratic behavior (2) of the local energies, the minimization (7) is expected to yield a well-posed linearly elastic problem with a unique solution within a sufficiently small neighborhood of $\bar{\mathbf{F}} = \mathbf{I}$. As the deformation progresses beyond the linearly elastic neighborhood into the finite deformation regime, the material may reach a point at which this unique solution bifurcates into different energy solutions. This point corresponds to the onset of an instability. The computation of all possible instabilities is a practically impossible task, especially for the random material systems of interest here. (In actuality, many of the instabilities may not even be relevant for our purposes since they may not lead to cavitating solutions.) In order to circumvent this problem, we will adopt a semi-inverse approach by restricting attention to certain subclasses of deformations χ which allow for cavitation phenomena but exclude complicated bifurcated solutions. In some sense, this strategy is a generalization of the semi-inverse approach originally proposed by Ball (1982) of restricting attention to radially symmetric deformations (i.e., $\chi(\mathbf{X}) = r(R)/R\mathbf{X}$ with $R = |\mathbf{X}|$) in the simpler context of hydrostatic loading conditions. More specifically, we will not consider the general minimization problem (7), but instead study the following restricted problem:

$$E^* = \min_{\mathbf{F} \in \mathcal{K}^*(\bar{\mathbf{F}})} \frac{1}{|\Omega_0|} \int_{\Omega_0} W(\mathbf{X}, \mathbf{F}) \, d\mathbf{X}, \quad (16)$$

where the minimization is now over a suitably restricted set \mathcal{K}^* of deformation gradient tensors that includes cavitating solutions but excludes complicated bifurcated solutions associated with other types of instabilities. The precise choice of the set \mathcal{K}^* will be dictated by the construction process described in Section 3 below. For notational simplicity, we will drop the use of the symbol $*$ in E^* henceforth, with the understanding that E will denote the total elastic energy defined in (16). By the same token, $\mathbf{F}(\mathbf{X})$ in expression (12) for f will denote henceforth the minimizing field in (16).

3. An iterated homogenization approach

In order to generate solutions for (16) and (12), we propose a “construction” strategy, one in which we devise a special, but yet sufficiently general, family of random microstructures θ_0 that permit the exact computation of the resulting homogenization problem. More specifically, our strategy comprises two main steps. The first step, described in Section 3.1, consists of an iterated homogenization procedure (or differential scheme) in finite elasticity that provides an exact solution for the total elastic energy of a class of two-phase solids in terms of an auxiliary dilute problem. The second step, described in Section 3.2, is concerned with the auxiliary dilute problem, which consists of the construction of a class of two-phase random microgeometries whose *matrix* phase is present in dilute proportions in such a way that their total elastic energy can be determined exactly and explicitly up to a set of nonlinear algebraic equations. Combining these two steps and specializing the result to the class of solids described in Section 2 leads to solutions for the total elastic energy E and the current volume fraction of cavities f , given directly in terms of $W^{(1)}$ and $W^{(2)}$, the one-point and two-point probabilities of the random distribution of cavities $p_0^{(2)}$ and $p_0^{(22)}$, and the applied loading conditions $\bar{\mathbf{F}}$. In turn, as discussed in Section 4, making use of these solutions in (13) provides the means of computing via (14)–(15) the onset of cavitation in large classes of materials, containing fairly general types of defects, under general 3D loading conditions.

3.1. Iterated homogenization in finite elasticity

Iterated homogenization methods, or differential schemes, are iterative processes that make use of results for the effective properties of *dilute* composites in order to generate corresponding results for composites with *finite* phase

volume fractions. This technique was originally reported in the 1930s in the context of electrostatics (Bruggeman, 1935), and ever since has repeatedly proved extremely helpful in deriving the macroscopic properties of *linear* composites with a wide range of random microstructures; see, e.g., Norris (1985), Avellaneda (1987), and Chapter 10.7 in the monograph by Milton (2002) and references therein. By contrast, its use for *nonlinear* composites has not been pursued to nearly the same extent, presumably because of the inherent technical difficulties. Nevertheless, the central idea of this technique is geometrical in nature and can therefore be applied to any constitutively nonlinear problem of choice; see, e.g., Duva (1984) and Idiart (2008) for applications to small-strain nonlinear elasticity.

In the context of finite elasticity, Lopez-Pamies (2010a) has recently proposed a differential scheme for two-phase solids. The starting point is to consider a class of material systems made up of two constituent phases, characterized by stored-energy functions $W^{(1)}$ and $W^{(2)}$, with geometrically similar microgeometries that are parameterized by the volume fraction of one of the constituent phases. Let that phase be $s=1$, for instance, and denote by $\alpha^{[1]}$ its volume fraction in this first iteration; throughout this subsection, phase volume fractions refer to the undeformed configuration, and a superscript $[k]$ is used to denote quantities associated with the k th iteration in the differential scheme. Now, within that class of microgeometries, consider a sequence of members with decreasing $\alpha^{[1]}$, and assume that the total elastic energy (or effective stored-energy function) $E^{[1]}$ associated with those microgeometries, as formally defined by (16), exhibits a polynomial asymptotic behavior as $\alpha^{[1]} \rightarrow 0$. We can thus write

$$E^{[1]}(\bar{\mathbf{F}}) = W^{(2)}(\bar{\mathbf{F}}) - \mathcal{H}[W^{(1)}, W^{(2)}; \bar{\mathbf{F}}] \alpha^{[1]} + O(\alpha^{[1]^2}), \quad (17)$$

where \mathcal{H} is a functional⁵ with respect to its first two arguments, $W^{(1)}$ and $W^{(2)}$, and a function with respect to its third argument $\bar{\mathbf{F}}$. The specific form of \mathcal{H} depends, of course, on the class of microgeometries being considered.⁶ Note, however, that the specific role of the “dilute” phase is at this stage immaterial. In this work, as will be elaborated in the next subsection, the role of the dilute phase will be played by the matrix phase — as opposed to the more standard inclusion phase — in a class of particulate microgeometries.

Next, consider the *same*⁷ class of two-phase microgeometries, where the “dilute” phase is again phase 1, but the “non-dilute” phase is characterized by the stored-energy function (17), rather than by $W^{(2)}$. Denote the volume fraction of phase 1 in this second iteration by $\alpha^{[2]}$, and, again, consider a sequence of microgeometries with decreasing $\alpha^{[2]}$. The effective stored-energy function associated with those microgeometries is, to first order in $\alpha^{[2]}$,

$$E^{[2]}(\bar{\mathbf{F}}) = E^{[1]}(\bar{\mathbf{F}}) - \mathcal{H}[W^{(1)}, E^{[1]}; \bar{\mathbf{F}}] \alpha^{[2]}, \quad (18)$$

where \mathcal{H} is the *same* functional as in (17). Note that the *total* volume fraction of phase 1 in this two-phase material is now $\alpha^{[2]} + \alpha^{[1]}(1 - \alpha^{[2]})$. Thus, an amount $\alpha^{[2]}(1 - \alpha^{[1]})$ of phase 1 has been added to the material in this second iteration.

It is apparent now that repeating the same above process $k+1$ times, where k is an arbitrarily large integer, generates a two-phase material with total elastic energy

$$E^{[k+1]}(\bar{\mathbf{F}}) = E^{[k]}(\bar{\mathbf{F}}) - \mathcal{H}[W^{(1)}, E^{[k]}; \bar{\mathbf{F}}] \alpha^{[k+1]}, \quad (19)$$

which contains a *total* volume fraction of phase 1 given by

$$c^{[k+1]} = 1 - \prod_{j=1}^{k+1} (1 - \alpha^{[j]}). \quad (20)$$

Furthermore, note that the *increment* in total volume fraction of phase 1 in this iteration (i.e., in passing from k to $k+1$) reads as

$$c^{[k+1]} - c^{[k]} = \prod_{j=1}^k (1 - \alpha^{[j]}) - \prod_{j=1}^{k+1} (1 - \alpha^{[j]}) = \alpha^{[k+1]} (1 - c^{[k]}), \quad (21)$$

from which it is a trivial matter to establish the following identity:

$$\alpha^{[k+1]} = \frac{c^{[k+1]} - c^{[k]}}{1 - c^{[k]}}. \quad (22)$$

Next, after substituting (22) in expression (19), we obtain

$$(1 - c^{[k]}) \frac{E^{[k+1]}(\bar{\mathbf{F}}) - E^{[k]}(\bar{\mathbf{F}})}{c^{[k+1]} - c^{[k]}} + \mathcal{H}[W^{(1)}, E^{[k]}; \bar{\mathbf{F}}] = 0. \quad (23)$$

⁵ That is, \mathcal{H} is an operator (e.g., a differential operator) with respect to the stored-energy functions $W^{(s)}$, so that it can depend, for instance, not just on $W^{(s)}$ but also on any derivative $\partial^n W^{(s)} / \partial \mathbf{F}^n$, $n \in \mathbb{N}$.

⁶ For the microgeometries considered in this work the functional \mathcal{H} will be given by (42).

⁷ The more general case of different dilute distributions — corresponding, for instance, to using different inclusion shapes and orientations — at each iteration will be studied in a future work.

This difference equation can be finally recast — upon using the facts that the increment $c^{[k+1]}-c^{[k]}$ is infinitesimally small and that k is arbitrarily large — as the following *initial-value problem*:

$$(1-c_0^{(1)}) \frac{\partial E}{\partial c_0^{(1)}} + \mathcal{H}[W^{(1)}, E; \bar{\mathbf{F}}] = 0, \quad E(\bar{\mathbf{F}}, 0) = W^{(2)}(\bar{\mathbf{F}}), \quad (24)$$

for the total elastic energy $E(\bar{\mathbf{F}}, c_0^{(1)})$, where $c_0^{(1)}$ denotes the total volume fraction of phase 1 in the final microgeometry. Alternatively, the energy E can be rewritten as a function of the initial volume fraction of phase 2 given by $c_0^{(2)} = 1 - c_0^{(1)}$. The resulting equation for $E(\bar{\mathbf{F}}, c_0^{(2)})$ is then given by

$$c_0^{(2)} \frac{\partial E}{\partial c_0^{(2)}} - \mathcal{H}[W^{(1)}, E; \bar{\mathbf{F}}] = 0, \quad E(\bar{\mathbf{F}}, 1) = W^{(2)}(\bar{\mathbf{F}}). \quad (25)$$

In summary, starting from the total elastic energy of any *dilute* microgeometry of choice, as determined by the functional \mathcal{H} , the above differential scheme yields an *exact* formulation (in the form of an initial-value problem) for the total elastic energy E of a material with *finite* values of phase volume fractions. For later reference, it is noted that if the dilute microgeometry is of particulate type, the above scheme generates non-dilute microgeometries that are also particulate. This follows from the fact that the same functional \mathcal{H} and the same dilute phase are used at each iteration step.

The usefulness of the exact formulation (25) then hinges upon being able to compute the functional \mathcal{H} describing the relevant dilute response of the material systems of interest. In general, it is *not* possible to solve dilute problems in *finite elasticity* by analytical means. This is in contrast to dilute problems in *linear elasticity* for which there is, for instance, the explicit solution of [Eshelby \(1957\)](#) and its generalizations. As detailed in the sequel, there is, however, a fairly general class of particulate microstructures for which the dilute response functional \mathcal{H} can be computed *exactly*⁸ and *explicitly*: sequential laminates ([deBotton, 2005](#); [Idiart, 2008](#)).

3.2. The auxiliary dilute microgeometries: sequential laminates

A sequential laminate is an iterative construction obtained by layering laminated materials (which in turn have been obtained from lower-order lamination procedures) with other laminated materials, or directly with the homogeneous phases that make up the composite, in such a way as to produce hierarchical microgeometries of increasing complexity (see, e.g., [Milton, 2002](#), Chapter 9). The *rank* of the laminate refers to the number of layering operations required to reach the final sequential laminate. Below, we follow a strategy similar to that formulated by [Idiart \(2008\)](#) in the context of small-strain nonlinear elasticity to compute the total elastic energy of a general class of two-phase nonlinear-elastic sequential laminates.

The starting point in constructing sequential laminates is to consider a simple, or rank-1, laminate with a given layering direction $\xi^{[1]}$, and with phases 1 and 2 in proportions $(1-\beta^{[1]})$ and $\beta^{[1]}$, respectively, as shown in [Fig. 3\(a\)](#); throughout this subsection, layering directions and volume fractions refer to the undeformed configuration, and a superscript $[i]$ is used to mark quantities associated with a rank- i laminate.⁹ The characteristic function θ_0 describing this rank-1 laminated microgeometry depends on \mathbf{X} only through the combination $\mathbf{X} \cdot \xi^{[1]}$. It then follows that the relevant Euler–Lagrange equations associated with (16) admit solutions consisting of *uniform-per-layer* deformation gradient fields (see, e.g., [Geymonat et al., 1993](#)). Thus, restricting the set of admissible fields to uniform-per-layer deformations (i.e., the set \mathcal{K}^* in (16)), and denoting the uniform deformation gradient in phase s by $\mathbf{F}^{(s)}$, continuity of the displacement field and boundary conditions require that

$$\mathbf{F}^{(1)} - \mathbf{F}^{(2)} = \boldsymbol{\omega}^{[1]} \otimes \xi^{[1]}, \quad (26)$$

$$(1-\beta^{[1]})\mathbf{F}^{(1)} + \beta^{[1]}\mathbf{F}^{(2)} = \bar{\mathbf{F}}, \quad (27)$$

for some arbitrary vector $\boldsymbol{\omega}^{[1]}$. Solving for the fields $\mathbf{F}^{(s)}$, we obtain

$$\mathbf{F}^{(1)} = \bar{\mathbf{F}} + \beta^{[1]}\boldsymbol{\omega}^{[1]} \otimes \xi^{[1]}, \quad (28)$$

$$\mathbf{F}^{(2)} = \bar{\mathbf{F}} - (1-\beta^{[1]})\boldsymbol{\omega}^{[1]} \otimes \xi^{[1]}, \quad (29)$$

so that the total elastic energy of the rank-1 laminate can be written as (see, e.g., [deBotton, 2005](#))

$$E^{[1]}(\bar{\mathbf{F}}) = \min_{\boldsymbol{\omega}^{[1]} \in \mathbb{R}^3} \{ (1-\beta^{[1]})W^{(1)}(\mathbf{F}^{(1)}) + \beta^{[1]}W^{(2)}(\mathbf{F}^{(2)}) \}. \quad (30)$$

The optimality condition with respect to $\boldsymbol{\omega}^{[1]}$ implies continuity of the traction vector across material interfaces in the deformed configuration. Given that the set of kinematically admissible fields has been restricted to uniform-per-layer fields, expression (30) corresponds to the unique exact effective stored-energy function up to the onset of the first instability. Beyond that point along a

⁸ Alternatively, an analytical solution for \mathcal{H} may be also obtained *approximately* by means of linear comparison methods ([Lopez-Pamies and Ponte Castañeda, 2006](#)); this latter approach has already proved fruitful to construct analytical estimates for the onset of cavitation in compressible isotropic solids ([Lopez-Pamies, 2009](#)).

⁹ The use of similar notation to that of Section 3.1 should not lead to confusion.

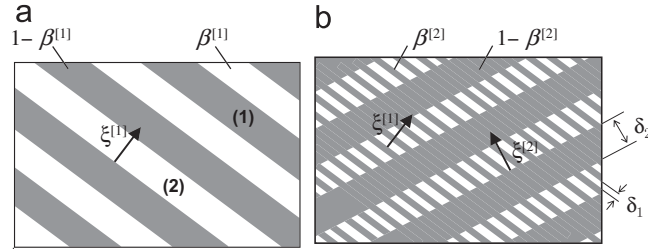


Fig. 3. Sequential laminates in their undeformed configurations: (a) simple or rank-1 laminate with lamination direction $\xi^{[1]}$, (b) rank-2 laminate with lamination direction $\xi^{[2]}$ ($\delta_2 \gg \delta_1$).

deformation path, other solutions that are not uniform per layer exist (Nestorovic and Triantafyllidis, 2004; Lopez-Pamies and Ponte Castañeda, 2009) that may correspond to lower overall energies, as already discussed in Section 2.

Sequential laminates are now constructed following an iterative process. Of all possible types of two-phase sequential laminates, we restrict attention to laminates formed by layering at every step a laminate with the homogeneous phase 1. A rank-2 laminate is thus constructed by layering the above rank-1 laminate with phase $s=1$, in proportions $\beta^{[2]}$ and $1-\beta^{[2]}$, respectively, along a certain layering direction $\xi^{[2]}$, as shown schematically in Fig. 3(b). The key assumption in this construction process is that the length scale of the *embedded* laminate is taken to be much smaller than the length scale of the *embedding* laminate, i.e., $\delta_1 \ll \delta_2$ in Fig. 3(b), so that in the rank-2 laminate, the rank-1 laminate can be regarded as a homogeneous phase. Consequently, the total elastic energy $E^{[2]}$ of the rank-2 laminate is given by an expression analogous to (30), with $W^{(2)}$ replaced by $E^{[1]}$. The total volume fraction of phase 2 in the rank-2 laminate is $\beta^{[1]}\beta^{[2]}$.

A rank- M laminate is obtained by repeating this process M times, always laminating a rank- m laminate with phase $s=1$, in proportions $\beta^{[m]}$ and $(1-\beta^{[m]})$, respectively, along a layering direction $\xi^{[m]}$. Making repeated use of the formula (30) for simple laminates, and after some algebraic manipulations, it is easy to show that the total elastic energy $E^{[M]}$ of the rank- M laminate is given by

$$E^{[M]}(\bar{\mathbf{F}}) = \min_{\substack{\omega^{[i]} \in \mathbb{R}^3 \\ i=1, \dots, M}} \left\{ v_0^{(2)} W^{(2)}(\bar{\mathbf{F}}^{(2)}) + \sum_{i=1}^M (1-\beta^{[i]}) \prod_{j=i+1}^M \beta^{[j]} W^{(1)}(\mathbf{F}^{[i]}) \right\}, \quad (31)$$

where $v_0^{(2)} = 1 - v_0^{(1)} = \prod_{i=1}^M \beta^{[i]}$ is the total volume fraction of phase 2, and the deformation gradient tensors $\mathbf{F}^{[i]}$ and $\bar{\mathbf{F}}^{(2)}$ are given by

$$\mathbf{F}^{[i]} = \bar{\mathbf{F}} + \beta^{[i]} \omega^{[i]} \otimes \xi^{[i]} - \sum_{j=i+1}^M (1-\beta^{[j]}) \omega^{[j]} \otimes \xi^{[j]}, \quad i=1, \dots, M, \quad (32)$$

$$\bar{\mathbf{F}}^{(2)} = \bar{\mathbf{F}} - \sum_{i=1}^M (1-\beta^{[i]}) \omega^{[i]} \otimes \xi^{[i]}. \quad (33)$$

Once again, note that each iteration step in the above construction process makes use of a set of kinematically admissible fields \mathcal{K}^* that is restricted to uniform-per-layer deformation gradients. From their construction process, it follows that these sequentially laminated microgeometries can be regarded as *random* and *particulate* with phase 2 playing the role of the “particle” (discontinuous) phase, surrounded by a (continuous) matrix made up of phase 1. It also follows that these microgeometries can be considered either as *monodisperse* or *polydisperse* in terms of the size of the “particles” made up of phase 2, since, rather remarkably, their size dispersion does not alter the total elastic energy (31). A further peculiar feature of these microgeometries, of particular importance in the sequel, is that the deformation gradient field within phase 2 is *uniform*. This is immediately recognizable from the fact that the stored-energy function $W^{(2)}$ appears in expression (31) evaluated at a single value of deformation given by (33). Within the matrix phase 1, by contrast, the deformation gradient field is non-uniform, taking on M different values given by (32).

The symmetry of sequentially laminated microgeometries can be increased by increasing the rank. However, extreme degrees of symmetry, such as for instance isotropy, can only be achieved in the limit of infinite rank. Now, taking the limit $M \rightarrow \infty$ directly in expression (31) is not straightforward due to the fact that $E^{[M]}$ depends on the order of the lamination sequence $\{(\beta^{[1]}, \xi^{[1]}), \dots, (\beta^{[M]}, \xi^{[M]})\}$. When the matrix phase is present in dilute volume fractions ($v_0^{(1)} \rightarrow 0$), however, such a dependence disappears and the limit can be easily evaluated. Indeed, motivated by the work of deBotton (2005), we consider “dilute” rank- M laminates characterized by volume fractions of the form

$$\beta^{[i]} = 1 - v^{[i]} v_0^{(1)} \quad \text{with } v^{[i]} \geq 0, \quad \sum_{i=1}^M v^{[i]} = 1, \quad (34)$$

where $v_0^{(1)}$ is an *infinitesimally small* quantity. Note that the constraint (34)₃ is such that the total volume fraction of the *matrix* phase in the undeformed configuration is precisely $v_0^{(1)}$, to first order. Furthermore, we take $\xi^{[i]} \neq \xi^{[j]}$ for all $i \neq j$.

A particular member in this class of microgeometries is thus specified by a set of constants $v^{[i]}$ and unit vectors $\xi^{[i]}$. Assuming that the expansion of the optimal $\omega^{[i]}$ for small $v_0^{(1)}$ is regular, and expanding terms inside the curly brackets in (31) about $v_0^{(1)} = 0$, we obtain the following expression for the total elastic energy to first order in $v_0^{(1)}$:

$$E^{[M]}(\bar{\mathbf{F}}) = \min_{\substack{\omega^{[i]} \in \mathbb{R}^3 \\ i = 1, \dots, M}} \left\{ (1 - v_0^{(1)})W^{(2)}(\bar{\mathbf{F}}) - v_0^{(1)} \sum_{i=1}^M v^{[i]} \left[\omega^{[i]} \cdot \frac{\partial W^{(2)}}{\partial \bar{\mathbf{F}}}(\bar{\mathbf{F}}) \xi^{[i]} - W^{(1)}(\bar{\mathbf{F}} + \omega^{[i]} \otimes \xi^{[i]}) \right] \right\}, \quad (35)$$

from which it is worth remarking that the contributions from each lamination i are decoupled. It is now convenient to introduce the generalized function

$$v(\xi) = \sum_{i=1}^M v^{[i]} \delta(\xi - \xi^{[i]}), \quad (36)$$

where $\delta(\xi)$ denotes the Dirac delta function. Expression (35) can then be rewritten as

$$E(\bar{\mathbf{F}}) = \min_{\omega(\xi)} \left\{ (1 - v_0^{(1)})W^{(2)}(\bar{\mathbf{F}}) - v_0^{(1)} \int_{|\xi|=1} \left[\omega \cdot \frac{\partial W^{(2)}}{\partial \bar{\mathbf{F}}}(\bar{\mathbf{F}}) \xi - W^{(1)}(\bar{\mathbf{F}} + \omega \otimes \xi) \right] v(\xi) d\xi \right\}, \quad (37)$$

where the minimization operation is now over vector functions

$$\omega : \mathcal{S} \rightarrow \mathbb{R}^3 \quad \text{with } \mathcal{S} = \{\xi \in \mathbb{R}^3 : |\xi| = 1\}, \quad (38)$$

and the superscript $[M]$ has been dropped to ease notation. This expression is valid for laminates of *finite* as well as *infinite* rank: in the first case, the function $v(\xi)$ is a sum of Dirac masses, while in the second case, it is a continuous function of ξ . In view of the constraint (34)₃, the function $v(\xi)$ always satisfies the constraint

$$\int_{|\xi|=1} v(\xi) d\xi = 1, \quad (39)$$

so that the operation

$$\langle \cdot \rangle \doteq \int_{|\xi|=1} (\cdot) v(\xi) d\xi \quad (40)$$

corresponds to a weighted orientational average. The result (37) can thus be finally written as

$$E(\bar{\mathbf{F}}) = W^{(2)}(\bar{\mathbf{F}}) - \mathcal{H}[W^{(1)}, W^{(2)}; \bar{\mathbf{F}}] v_0^{(1)} \quad (41)$$

with

$$\mathcal{H}[W^{(1)}, W^{(2)}; \bar{\mathbf{F}}] = W^{(2)}(\bar{\mathbf{F}}) + \max_{\omega(\xi)} \left\langle \omega \cdot \frac{\partial W^{(2)}}{\partial \bar{\mathbf{F}}}(\bar{\mathbf{F}}) \xi - W^{(1)}(\bar{\mathbf{F}} + \omega \otimes \xi) \right\rangle. \quad (42)$$

This expression constitutes an asymptotically exact result for the total elastic energy of a two-phase infinite-rank laminate where phase 1 is present in *dilute* volume fraction. Again, the microstructure of this laminate is random and particulate with phase 1 playing the role of the matrix material and phase 2 playing the role of the “particle” material. The distribution of phase 2 is characterized by the function $v(\xi)$, which will be directly related to the two-point probability function (5) further below. In passing, it is also interesting to remark that the above-constructed microstructure with dilute matrix phase is very much similar to the microstructures considered by Bourdin and Khon (2008) in the context of the topological optimization of high-porosity linearly elastic foams. These authors showed that in the high-porosity limit these laminates can be regarded as intersecting families of parallel walls.

3.3. The total elastic energy E and current volume fraction of cavities f

We are now in a position to construct solutions for (16) and (12) by combining the independent results developed in the two preceding subsections. Focusing first on expression (41), it is observed that the total elastic energy for the dilute microgeometries constructed in Section 3.2 is of the regular form (17) assumed in the differential scheme of Section 3.1 (namely, linear in $v_0^{(1)}$), with the functional \mathcal{H} given by (42). Then, by making use of (42) in (25) and identifying $c_0^{(2)}$ with f_0 , it is a simple matter to deduce that a solution for the total elastic energy $E = E(\bar{\mathbf{F}}, f_0)$ is given implicitly by the following first-order *nonlinear* partial differential equation (pde):

$$f_0 \frac{\partial E}{\partial f_0} - E - \max_{\omega(\xi)} \left\langle \omega \cdot \frac{\partial E}{\partial \bar{\mathbf{F}}} \xi - W^{(1)}(\bar{\mathbf{F}} + \omega \otimes \xi) \right\rangle = 0 \quad (43)$$

subject to the initial condition

$$E(\bar{\mathbf{F}}, 1) = W^{(2)}(\bar{\mathbf{F}}). \quad (44)$$

Having computed the solution (in the form of a first-order pde) (43) for (16), the associated volume fraction of cavities (12) in the deformed configuration can then be readily computed from well-known perturbation techniques (see, e.g., [Idiart](#)

and Ponte Castañeda, 2006). For the problem at hand, as detailed in Appendix A, $f = f(\bar{\mathbf{F}}, f_0)$ can be shown to be the solution of the following first-order linear pde:

$$f_0 \frac{\partial f}{\partial f_0} - (1 + \bar{\mathbf{F}}^{-T} \cdot \langle \boldsymbol{\omega} \otimes \boldsymbol{\xi} \rangle) f - \frac{\partial f}{\partial \bar{\mathbf{F}}} \cdot \langle \boldsymbol{\omega} \otimes \boldsymbol{\xi} \rangle = 0, \quad (45)$$

where $\boldsymbol{\omega}$ is the maximizing vector in (43), subject to the initial condition

$$f(\bar{\mathbf{F}}, 1) = 1. \quad (46)$$

Expressions (43)–(44) and (45)–(46) constitute *exact* results for the total elastic energy (16) and current volume fraction of cavities (12) of a material system made up of a nonlinear elastic solid, with stored-energy function $W^{(1)}$, containing a specific class of random distributions of disconnected cavities, with mechanical properties characterized by the stored-energy function $W^{(2)}$. These results depend on the microstructure through the initial volume fraction f_0 of cavities and the function $v(\boldsymbol{\xi})$. While the volume fraction corresponds exactly to the one-point probability (4), the function $v(\boldsymbol{\xi})$ is directly related to the two-point probability (5) — which, again, contains information about the shape and spatial distribution of the cavities — via the relation:

$$v(\boldsymbol{\xi}) = - \frac{1}{8\pi^2} \frac{\partial^2 h^*}{\partial p^2}(p, \boldsymbol{\xi}) \Big|_{p=0} \quad \text{with } h^*(p, \boldsymbol{\xi}) = \int_{\mathbb{R}^3} h(\mathbf{X}) \delta(\boldsymbol{\xi} \cdot \mathbf{X} - p) \, d\mathbf{X}, \quad (47)$$

where h^* is the Radon transform of the two-point correlation function h defined in (5). The derivation of the connection (47) is given in Appendix B.

4. Cavitation criterion

The results (43)–(44) and (45)–(46) for the total elastic energy E and current volume fraction of cavities f are valid for any value of initial volume fraction of cavities in the physical range $f_0 \in [0, 1]$. It is their asymptotic behavior in the limit as $f_0 \rightarrow 0+$ that is of interest here to analyze cavitation. Making use of the formal expressions (13)–(15) put forward in Section 2, we can finally postulate the criterion that follows:

The onset of cavitation in a nonlinear elastic material with stored-energy function $W^{(1)}$ containing a random distribution of defects with stored-energy function $W^{(2)}$ occurs at critical deformations $\bar{\mathbf{F}}_{cr}$ such that

$$\bar{\mathbf{F}}_{cr} \in \partial \mathcal{Z}[f, (\bar{\mathbf{F}})] \quad \text{and} \quad 0 < \|\bar{\mathbf{S}}_*(\bar{\mathbf{F}}_{cr})\| < +\infty, \quad (48)$$

where

$$f_*(\bar{\mathbf{F}}) \doteq \lim_{f_0 \rightarrow 0+} f(\bar{\mathbf{F}}, f_0) \quad \text{and} \quad \bar{\mathbf{S}}_*(\bar{\mathbf{F}}) \doteq \lim_{f_0 \rightarrow 0+} \frac{\partial E}{\partial \bar{\mathbf{F}}}(\bar{\mathbf{F}}, f_0). \quad (49)$$

Here, $E(\bar{\mathbf{F}}, f_0)$ and $f(\bar{\mathbf{F}}, f_0)$ are the functions defined by (43)–(44) and (45)–(46), and $\partial \mathcal{Z}[f, (\bar{\mathbf{F}})]$ denotes the boundary of the zero set of $f_*(\bar{\mathbf{F}})$. The corresponding first Piola–Kirchhoff and Cauchy critical stresses at cavitation are given respectively by

$$\bar{\mathbf{S}}_{cr} = \bar{\mathbf{S}}_*(\bar{\mathbf{F}}_{cr}) \quad \text{and} \quad \bar{\mathbf{T}}_{cr} = \bar{\mathbf{J}}_{cr}^{-1} \bar{\mathbf{S}}_{cr} \bar{\mathbf{F}}_{cr}^T, \quad (50)$$

where $\bar{\mathbf{J}}_{cr} = \det \bar{\mathbf{F}}_{cr}$.

The following comments are in order:

- (i) *Loading conditions*: Results (43)–(46) are valid for arbitrary deformations $\bar{\mathbf{F}}$. Accordingly, the criterion (48)–(50) provides a framework to study cavitation under general 3D loading conditions with arbitrary triaxiality.
- (ii) *Material behavior of the solid and of the defects*: Expressions (43)–(46) apply to any matrix stored-energy function $W^{(1)}$ and to any cavity stored-energy function $W^{(2)}$, provided that these satisfy usual physically based mathematical requirements. Thus, the criterion (48)–(50) allows for the study of cavitation in virtually any nonlinear elastic solid of choice, including compressible and anisotropic solids. Moreover, this formulation can be used to investigate the effect of pressurized (and even more complex types of nonlinear elastic) defects on cavitation.
- (iii) *Geometry and spatial distribution of defects*: Within the specific geometric class of cavities considered, the results (43)–(46) are valid for arbitrary two-point statistical information describing the initial shape and spatial location of the underlying cavities, as dictated by relation (47). The proposed criterion (48)–(50) permits therefore to directly account for and to study the effects of the initial geometry and spatial distribution of defects on the occurrence of cavitation.
- (iv) *Interaction among defects*: By construction, the underlying defects in the criterion (48)–(50) interact in such a manner that they deform *uniformly* under any applied deformation $\bar{\mathbf{F}}$; a proof of this feature is provided in Appendix C. While this is certainly a special type of interaction, we expect other interactions associated with different distributions of defects to lead to similar onset-of-cavitation results. This expectation is supported by the comparisons with finite-element results for the sudden growth of isolated spherical defects in Neo-Hookean materials presented in the

companion paper (Lopez-Pamies et al., in press). Further evidence supporting this expectation has been provided by the recent work of Xu and Henao, in press), who have shown via some examples that the critical load at which cavitation ensues based on the growth of an isolated circular defect is essentially the same as that based on the growth of two neighboring circular defects. It is important to emphasize, however, that differences in the interactions among defects will play a crucial role in the post-cavitation regime, wherein defects grow into finite sizes and may even possibly coalesce.

- (v) *Mathematical tractability*: The pdes (43) and (45) correspond to Hamilton–Jacobi equations where the initial volume fraction of cavities f_0 and the macroscopic deformation gradient $\bar{\mathbf{F}}$ play the role of “time” and “space” variables, respectively. Due to the prominent role of Hamilton–Jacobi equations in physics, a substantial body of literature exists on efficient analytical and numerical techniques for solving this type of equations (see, e.g., Benton, 1977; Polyaniin et al., 2002). Hence, in spite of its generality, the proposed criterion (48)–(50) is fairly tractable and thus expected to be useful for generating explicit results for the onset of cavitation in nonlinear elastic solids. As a first application, we have worked out in a companion paper (Lopez-Pamies et al., in press) an *explicit* result for the onset of cavitation in Neo-Hookean solids containing an isotropic distribution of vacuous defects.
- (vi) *Connection with the classical result of Ball for radially symmetric cavitation*: For the special case of hydrostatic loading conditions, isotropic solids, and defects that are vacuous and isotropically distributed, the criterion (48)–(50) recovers Ball’s classical result for the critical pressure at which cavitation ensues in a unit ball made up of isotropic material under hydrostatic loading. (The reason for this agreement is partly due to the fact that the deformation in the defects in the formulation (43)–(46) is uniform, exactly as the deformation in the cavity of a radially deformed spherical shell.) The relevant details of this connection are provided in Section 5, but here we remark that its main implication is that the criterion (48)–(50) can be thought of as an extension of the classical result of Ball to deal with non-symmetric loading conditions, compressible anisotropic materials, and fairly general types of defects.

In the next subsections, we discuss the specializations of the criterion (48)–(50) to three cases of practical interest: incompressible solids, isotropic solids containing an isotropic distribution of defects, and hydrostatic loading conditions.

4.1. Incompressible solids

In the case of incompressible solids $W^{(1)}(\mathbf{F}) = +\infty$ if $\det \mathbf{F} \neq 1$, and so the maximizing condition in (43) can be simplified. Indeed, if the matrix phase is incompressible, the argument of $W^{(1)}$ in (43) must have determinant equal to one. Now,

$$\det(\bar{\mathbf{F}} + \boldsymbol{\omega} \otimes \boldsymbol{\xi}) = \det \bar{\mathbf{F}} \det(\mathbf{I} + \bar{\mathbf{F}}^{-1} \boldsymbol{\omega} \otimes \boldsymbol{\xi}) = \bar{J} [1 + \boldsymbol{\omega} \cdot \bar{\mathbf{F}}^{-T} \boldsymbol{\xi}], \quad (51)$$

and therefore the constraint

$$\boldsymbol{\omega} \cdot \bar{\mathbf{F}}^{-T} \boldsymbol{\xi} = \frac{1 - \bar{J}}{\bar{J}}, \quad (52)$$

where it is recalled that $\bar{J} = \det \bar{\mathbf{F}}$, must be satisfied. This relation implies that the vector $\boldsymbol{\omega}$ is expressible in the form

$$\boldsymbol{\omega} = \frac{1 - \bar{J}}{\bar{J}} \bar{\mathbf{F}} \boldsymbol{\xi} + \mathbf{u}, \quad (53)$$

where

$$\mathbf{u} : \mathcal{S} \rightarrow \mathcal{Q} \quad \text{with } \mathcal{S} = \{\boldsymbol{\xi} \in \mathbb{R}^3 : |\boldsymbol{\xi}| = 1\} \text{ and } \mathcal{Q} = \{\mathbf{v} \in \mathbb{R}^3 : \bar{\mathbf{F}}^{-T} \boldsymbol{\xi} \cdot \mathbf{v} = 0\}. \quad (54)$$

That is, \mathbf{u} is a vector function of $\boldsymbol{\xi}$ that lies in the plane defined by the normal $\bar{\mathbf{F}}^{-T} \boldsymbol{\xi}$.

A direct consequence of the above restriction is that the initial-value problem (43)–(44) for the total elastic energy E can be simplified to

$$f_0 \frac{\partial E}{\partial f_0} - E - \max_{\mathbf{u}(\boldsymbol{\xi})} \left\langle \left[\frac{1 - \bar{J}}{\bar{J}} \bar{\mathbf{F}} \boldsymbol{\xi} + \mathbf{u} \right] \cdot \frac{\partial E}{\partial \bar{\mathbf{F}}} \boldsymbol{\xi} - W^{(1)} \left(\bar{\mathbf{F}} + \frac{1 - \bar{J}}{\bar{J}} \bar{\mathbf{F}} \boldsymbol{\xi} \otimes \boldsymbol{\xi} + \mathbf{u} \otimes \boldsymbol{\xi} \right) \right\rangle = 0, \quad E(\bar{\mathbf{F}}, 1) = W^{(2)}(\bar{\mathbf{F}}), \quad (55)$$

where it is emphasized that the original optimization over *three-dimensional* vectors $\boldsymbol{\omega}$ is now replaced by the optimization over “*two-dimensional*” vectors \mathbf{u} . Another direct implication of the incompressibility of the matrix phase is that the current volume fraction of cavities f must depend on the applied deformation gradient $\bar{\mathbf{F}}$ only through its determinant \bar{J} , a restriction that allows simplifying the initial-value problem (45)–(46) to

$$f_0 \frac{\partial f}{\partial f_0} - \left(1 + \frac{1 - \bar{J}}{\bar{J}} \right) f - (1 - \bar{J}) \frac{\partial f}{\partial \bar{J}} = 0, \quad f(\bar{\mathbf{F}}, 1) = 1. \quad (56)$$

The pde (56)₁, subject to the condition (56)₂, admits the following closed-form solution:

$$f = \frac{\bar{J} - 1}{\bar{J}} + \frac{f_0}{\bar{J}}, \quad (57)$$

which is nothing more than a plain conservation-of-mass statement for the *incompressible* matrix phase, as expected physically.

Having determined relations (55) and (57) for the case of incompressible solids with arbitrary values of initial volume fraction of cavities $f_0 \in [0, 1]$, we focus next on the computation of f_* and $\bar{\mathbf{S}}_*$, as defined by expressions (49). From (49)₁, it is trivial to deduce that

$$f_*(\bar{\mathbf{F}}) = \frac{\bar{J}-1}{\bar{J}}. \quad (58)$$

The computation of $\bar{\mathbf{S}}_*$, on the other hand, does not admit a generic simplification, since the asymptotic form of E as $f_0 \rightarrow 0+$ can widely vary depending on the specific choice of stored-energy functions $W^{(1)}$ and $W^{(2)}$. At any rate, by making use of (58) in (48), it is a simple matter to deduce that for incompressible solids cavitation ensues at critical deformations $\bar{\mathbf{F}}_{cr}$ such that

$$\bar{\mathbf{F}}_{cr} \in \partial \mathcal{Z}[f_*(\bar{\mathbf{F}})] = \{\bar{\mathbf{F}} : \bar{J} = 1\} \quad \text{and} \quad 0 < \|\bar{\mathbf{S}}_*(\bar{\mathbf{F}}_{cr})\| < +\infty. \quad (59)$$

and at corresponding first Piola–Kirchhoff and Cauchy critical stresses

$$\bar{\mathbf{S}}_{cr} = \bar{\mathbf{S}}_*(\bar{\mathbf{F}}_{cr}) \quad \text{and} \quad \bar{\mathbf{T}}_{cr} = \bar{\mathbf{S}}_{cr} \bar{\mathbf{F}}_{cr}^T. \quad (60)$$

Thus, as expected, cavitation can only occur at *isochoric* deformations, irrespectively of the type of incompressible solid ($W^{(1)}$) and defects ($W^{(2)}$) being considered. The critical stresses at which cavitation takes place, by contrast, will strongly depend on the specific choice of solid ($W^{(1)}$) and type and distribution of defects ($W^{(2)}$ and $v(\xi)$), as determined by the asymptotic solution of (43)–(44) in the limit as $f_0 \rightarrow 0+$. An example of such a solution is given in the companion paper (Lopez-Pamies et al., *in press*), where we work out the loci of critical stresses at which cavitation ensues in incompressible Neo-Hookean solids.

4.2. Isotropic solids with isotropic distributions of defects

When the initial distribution of defects is isotropic and the mechanical response of the solid and the defects is also isotropic, geometric and constitutive hypotheses of notable practical importance, the formulation (43)–(46) can be simplified significantly. For this class of material systems the microstructural function $v(\xi)$ takes the simple form (see Appendix B)

$$v(\xi) = \frac{1}{4\pi} \quad (61)$$

and the stored-energy functions $W^{(s)}$ can be conveniently expressed as symmetric functions of the eigenvalues (or principal stretches) $\lambda_1, \lambda_2, \lambda_3$ of $(\mathbf{F}^T \mathbf{F})^{1/2}$:

$$W^{(s)}(\mathbf{F}) = \phi^{(s)}(\lambda_1, \lambda_2, \lambda_3) \quad (62)$$

($s=1,2$), where $\phi^{(s)}$ are symmetric. In view of (61) and (62), it follows that the total elastic energy E and current volume fraction of cavities f are isotropic functions of $\bar{\mathbf{F}}$ so that we can write

$$E(\bar{\mathbf{F}}, f_0) = \tilde{E}(\bar{\lambda}_1, \bar{\lambda}_2, \bar{\lambda}_3, f_0) \quad \text{and} \quad f(\bar{\mathbf{F}}, f_0) = \tilde{f}(\bar{\lambda}_1, \bar{\lambda}_2, \bar{\lambda}_3, f_0), \quad (63)$$

where the scalar functions \tilde{E} and \tilde{f} are symmetric in their first three arguments, and the notation $\bar{\lambda}_1, \bar{\lambda}_2, \bar{\lambda}_3$ has been introduced to denote the eigenvalues of the macroscopic deformation-measure $(\bar{\mathbf{F}}^T \bar{\mathbf{F}})^{1/2}$. Because E and f only depend on $\bar{\mathbf{F}}$ through the principal stretches, it suffices to restrict attention, without loss of generality, to pure stretch loadings of the diagonal form

$$\bar{F}_{ij} = \text{diag}(\bar{\lambda}_1, \bar{\lambda}_2, \bar{\lambda}_3). \quad (64)$$

Given the above geometric (61), constitutive (62), and loading (64) restrictions, the Hamilton–Jacobi equation (43) for E can be recast as the simpler Hamilton–Jacobi equation

$$f_0 \frac{\partial \tilde{E}}{\partial f_0} - \tilde{E} - \max_{\omega(\xi)} \int_{|\xi|=1} \frac{1}{4\pi} \left[\sum_{p=1}^3 \frac{\partial \tilde{E}}{\partial \bar{\lambda}_p} \omega_p \xi_p - \phi^{(1)}(\gamma_1, \gamma_2, \gamma_3) \right] d\xi = 0 \quad (65)$$

for \tilde{E} , while the associated initial condition (44) can be recast as

$$\tilde{E}(\bar{\lambda}_1, \bar{\lambda}_2, \bar{\lambda}_3, 1) = \phi^{(2)}(\bar{\lambda}_1, \bar{\lambda}_2, \bar{\lambda}_3). \quad (66)$$

In (65), $\gamma_1, \gamma_2, \gamma_3$ are the eigenvalues of $[(\bar{\mathbf{F}} + \omega \otimes \xi)^T (\bar{\mathbf{F}} + \omega \otimes \xi)]^{1/2}$, as defined by the three positive roots of the characteristic equation

$$\gamma^6 - \mathcal{I}_1 \gamma^4 + \mathcal{I}_2 \gamma^2 - \mathcal{I}_3 = 0, \quad (67)$$

where

$$\begin{aligned} \mathcal{I}_1 &= \bar{\lambda}_1^2 + \bar{\lambda}_2^2 + \bar{\lambda}_3^2 + (2\bar{\lambda}_1 \bar{\xi}_1 + \omega_1)\omega_1 + (2\bar{\lambda}_2 \bar{\xi}_2 + \omega_2)\omega_2 + (2\bar{\lambda}_3 \bar{\xi}_3 + \omega_3)\omega_3, \\ \mathcal{I}_2 &= \bar{\lambda}_1^2 \bar{\lambda}_2^2 + \bar{\lambda}_1^2 \bar{\lambda}_3^2 + \bar{\lambda}_2^2 \bar{\lambda}_3^2 + 2(\bar{\lambda}_2^2 + \bar{\lambda}_3^2)\bar{\lambda}_1 \bar{\xi}_1 \omega_1 + 2(\bar{\lambda}_1^2 + \bar{\lambda}_3^2)\bar{\lambda}_2 \bar{\xi}_2 \omega_2 + 2(\bar{\lambda}_1^2 + \bar{\lambda}_2^2)\bar{\lambda}_3 \bar{\xi}_3 \omega_3 \\ &\quad + \bar{\lambda}_3^2 (\bar{\xi}_1^2 + \bar{\xi}_2^2)(\omega_1^2 + \omega_2^2) + \bar{\lambda}_2^2 (\bar{\xi}_1^2 + \bar{\xi}_3^2)(\omega_1^2 + \omega_3^2) + \bar{\lambda}_1^2 (\bar{\xi}_2^2 + \bar{\xi}_3^2)(\omega_2^2 + \omega_3^2) \\ &\quad + 2\bar{\lambda}_1 \bar{\lambda}_2 \bar{\xi}_1 \bar{\xi}_2 \omega_1 \omega_2 + 2\bar{\lambda}_1 \bar{\lambda}_3 \bar{\xi}_1 \bar{\xi}_3 \omega_1 \omega_3 + 2\bar{\lambda}_2 \bar{\lambda}_3 \bar{\xi}_2 \bar{\xi}_3 \omega_2 \omega_3, \\ \mathcal{I}_3 &= (\bar{\lambda}_1 \bar{\lambda}_2 \bar{\lambda}_3 + \bar{\lambda}_2 \bar{\lambda}_3 \bar{\xi}_1 \omega_1 + \bar{\lambda}_1 \bar{\lambda}_3 \bar{\xi}_2 \omega_2 + \bar{\lambda}_1 \bar{\lambda}_2 \bar{\xi}_3 \omega_3)^2. \end{aligned} \quad (68)$$

Similarly, the Hamilton–Jacobi equation (45) for the current volume fraction of cavities can be rewritten in the form

$$f_0 \frac{\partial \tilde{f}}{\partial f_0} - \left[1 + \frac{1}{4\pi} \int_{|\xi|=1} \sum_{p=1}^3 \bar{\lambda}_p^{-1} \omega_p \xi_p \, d\xi \right] \tilde{f} - \frac{1}{4\pi} \int_{|\xi|=1} \sum_{p=1}^3 \frac{\partial \tilde{f}}{\partial \lambda_p} \omega_p \xi_p \, d\xi = 0, \quad (69)$$

where ω denotes the maximizing vector in (65), which is subject to the initial condition

$$\tilde{f}(\bar{\lambda}_1, \bar{\lambda}_2, \bar{\lambda}_3, 1) = 1. \quad (70)$$

If the solid is isotropic and, in addition, *incompressible* (namely, $\phi^{(1)}(\lambda_1, \lambda_2, \lambda_3) = +\infty$ if $\lambda_1 \lambda_2 \lambda_3 \neq 1$) the initial-value problem (65)–(66) specializes further to

$$f_0 \frac{\partial \tilde{E}}{\partial f_0} - \tilde{E} - \max_{\mathbf{u}(\xi)} \int_{|\xi|=1} \frac{1}{4\pi} \left[\sum_{p=1}^3 \frac{\partial \tilde{E}}{\partial \lambda_p} \omega_p \xi_p - \phi^{(1)}(\gamma_1, \gamma_2, \gamma_3) \right] d\xi = 0, \quad \tilde{E}(\bar{\lambda}_1, \bar{\lambda}_2, \bar{\lambda}_3, 1) = \phi^{(2)}(\bar{\lambda}_1, \bar{\lambda}_2, \bar{\lambda}_3) \quad (71)$$

with

$$\omega_1 = \frac{1 - \bar{\lambda}_1 \bar{\lambda}_2 \bar{\lambda}_3}{\bar{\lambda}_2 \bar{\lambda}_3} \bar{\xi}_1 + u_1, \quad \omega_2 = \frac{1 - \bar{\lambda}_1 \bar{\lambda}_2 \bar{\lambda}_3}{\bar{\lambda}_1 \bar{\lambda}_3} \bar{\xi}_2 + u_2, \quad \omega_3 = \frac{1 - \bar{\lambda}_1 \bar{\lambda}_2 \bar{\lambda}_3}{\bar{\lambda}_1 \bar{\lambda}_2} \bar{\xi}_3 + u_3, \quad (72)$$

where the components of the vector \mathbf{u} satisfy the constraint

$$\frac{1}{\bar{\lambda}_1} \bar{\xi}_1 u_1 + \frac{1}{\bar{\lambda}_2} \bar{\xi}_2 u_2 + \frac{1}{\bar{\lambda}_3} \bar{\xi}_3 u_3 = 0, \quad (73)$$

as dictated by relations (54), and where the eigenvalues $\gamma_1, \gamma_2, \gamma_3$ are still defined by the three positive roots of (67). Moreover, as already discussed in the more general context of Section 4.1, the initial-value problem (69)–(70) admits the closed-form solution

$$\tilde{f}(\bar{\lambda}_1, \bar{\lambda}_2, \bar{\lambda}_3, f_0) = \frac{\bar{\lambda}_1 \bar{\lambda}_2 \bar{\lambda}_3 - 1}{\bar{\lambda}_1 \bar{\lambda}_2 \bar{\lambda}_3} + \frac{f_0}{\bar{\lambda}_1 \bar{\lambda}_2 \bar{\lambda}_3}. \quad (74)$$

In short, for the case of isotropic materials with isotropic distribution of defects, the “space” dimension in Eqs. (65), (69), and (71)₁ reduces from nine (i.e., the nine components of \tilde{F}_{ij}) to three (i.e., the three principal stretches $\bar{\lambda}_1, \bar{\lambda}_2, \bar{\lambda}_3$). This simplifies considerably the computation of the functions f , and $\bar{\mathbf{S}}$, in (49), and hence the computation of the onset of cavitation as determined by the criterion (48)–(50).

4.3. Hydrostatic loading conditions

Because of its particular physical relevance, and for later reference, we consider next the specialization of the proposed formulation to hydrostatic loading conditions with

$$\bar{\mathbf{F}} = \bar{\lambda} \mathbf{I}, \quad (75)$$

where $\bar{\lambda}$ is a positive loading parameter that takes the value 1 in the undeformed configuration. For simplicity, we restrict attention to the special case of isotropic solids, with stored-energy function of the form

$$W^{(1)}(\mathbf{F}) = \phi^{(1)}(\lambda_1, \lambda_2, \lambda_3), \quad (76)$$

that contain a random isotropic distribution of vacuous defects, so that

$$v(\xi) = \frac{1}{4\pi} \quad \text{and} \quad W^{(2)}(\mathbf{F}) = 0. \quad (77)$$

Then, according to the results of Section 4.2, we can write

$$E(\bar{\mathbf{F}}, f_0) = \tilde{E}(\bar{\lambda}, \bar{\lambda}, \bar{\lambda}, f_0) \doteq \tilde{E}(\bar{\lambda}, f_0) \quad \text{and} \quad f(\bar{\mathbf{F}}, f_0) = \tilde{f}(\bar{\lambda}, \bar{\lambda}, \bar{\lambda}, f_0) \doteq \tilde{f}(\bar{\lambda}, f_0) \quad (78)$$

for the total elastic energy and current volume fraction of cavities of the material, respectively. Now, because of the overall isotropy of the problem, the maximizing vector in (65) must be of the form $\omega = \omega \xi$ with $\omega \in \mathbb{R}$, which implies that the eigenvalues defined by (67) are simply given by $\gamma_1 = \bar{\lambda} + \omega$ and $\gamma_2 = \gamma_3 = \bar{\lambda}$, and hence that the Hamilton–Jacobi

equation (65) and associated initial condition (66) for the total elastic energy eventually reduce to

$$f_0 \frac{\partial \check{E}}{\partial f_0} - \check{E} - \max_{\omega} \left\{ \frac{\omega}{3} \frac{\partial \check{E}}{\partial \bar{\lambda}} - \phi^{(1)}(\bar{\lambda} + \omega, \bar{\lambda}, \bar{\lambda}) \right\} = 0, \quad \check{E}(\bar{\lambda}, 1) = 0. \quad (79)$$

Here, we remark that the maximizing condition in (79) is given by

$$\phi_1^{(1)}(\bar{\lambda} + \omega, \bar{\lambda}, \bar{\lambda}) = \frac{1}{3} \frac{\partial \check{E}}{\partial \bar{\lambda}}, \quad (80)$$

which is a nonlinear algebraic equation for ω . In this regard, given that (80) may have more than one root, it is emphasized that ω should be chosen as the root in (80) that maximizes the argument inside the curly brackets in (79). In expression (80) and below, $\phi_i^{(1)}$ denotes differentiation of $\phi^{(1)}$ with respect to its i th argument. Similarly, the current volume fraction of cavities (69) and corresponding initial condition (70) can be shown to reduce to

$$f_0 \frac{\partial \check{f}}{\partial f_0} - \left(1 + \frac{\omega}{\bar{\lambda}} \right) \check{f} - \frac{\omega}{3} \frac{\partial \check{f}}{\partial \bar{\lambda}} = 0, \quad \check{f}(\bar{\lambda}, 1) = 1, \quad (81)$$

where it is emphasized that ω here is the maximizing scalar in (79).

Further simplifications will depend on the particular choice of energy function $\phi^{(1)}$. For the special case of *incompressible* materials such that $\phi^{(1)}(\lambda_1, \lambda_2, \lambda_3) = +\infty$ if $\lambda_1 \lambda_2 \lambda_3 \neq 1$, the kinematical constraint (72)–(73) dictates that the maximizing scalar ω in (79) must be given by

$$\omega = \frac{1}{\bar{\lambda}^2} - \bar{\lambda}. \quad (82)$$

This simple form for ω allows to solve for the total elastic energy (79) and current volume fraction of cavities (81) in closed form. The solutions read as

$$\check{E}(\bar{\lambda}, f_0) = 3(\bar{\lambda}^3 - 1) \int_{\bar{\lambda}}^{(1 + (\bar{\lambda}^3 - 1)/f_0)^{1/3}} \frac{z^2}{(z^3 - 1)^2} \phi^{(1)}(z^{-2}, z, z) dz \quad (83)$$

and

$$\check{f}(\bar{\lambda}, f_0) = \frac{\bar{\lambda}^3 - 1}{\bar{\lambda}^3} + \frac{f_0}{\bar{\lambda}^3}, \quad (84)$$

respectively. The corresponding functions f_* and $\bar{\mathbf{S}}_*$ as defined by expressions (49) are then given by

$$f_*(\bar{\lambda} \mathbf{I}) = \frac{\bar{\lambda}^3 - 1}{\bar{\lambda}^3} \quad \text{and} \quad \bar{\mathbf{S}}_*(\bar{\lambda} \mathbf{I}) = P_*(\bar{\lambda}) \mathbf{I} \quad \text{with} \quad P_*(\bar{\lambda}) = \int_{\bar{\lambda}}^{\infty} \frac{\bar{\lambda}^2}{z^3 - 1} \frac{d\phi^{(1)}}{dz}(z^{-2}, z, z) dz. \quad (85)$$

Making direct use of these expressions in the criterion (48)–(50), it is then a simple matter to conclude that cavitation in an isotropic, incompressible nonlinear elastic material containing a random isotropic distribution of vanishingly small vacuous defects that is subjected to hydrostatic loading takes place at critical values $\bar{\lambda}_{cr}$ and P_{cr} of deformation $\bar{\lambda}$ and hydrostatic pressure¹⁰ P given by

$$\bar{\lambda}_{cr} = 1 \quad \text{and} \quad P_{cr} = P_*(\bar{\lambda}_{cr}) = \int_1^{\infty} \frac{1}{z^3 - 1} \frac{d\phi^{(1)}}{dz}(z^{-2}, z, z) dz. \quad (86)$$

Interestingly, this result agrees identically with the classical formula of Ball for radially symmetric cavitation of isotropic *incompressible* solids (cf. Ball, 1982, Eq. (1.10)). This agreement holds in fact true more generally for isotropic *compressible* solids — for which, unfortunately, there is no general explicit formula for the critical pressure at which cavitation ensues (see Ball, 1982, Section 7). Examining the nature and implications of this remarkable connection is the subject of the next section.

5. Connection with the classical result of Ball for radially symmetric cavitation

The majority of available results for cavitation in elastomeric solids — as initially formalized by Ball (1982) — are based on the solution for the radially symmetric deformation of a unit spherical shell made up of nonlinear elastic material under external hydrostatic loading. In this section, we recall such a solution and establish its intimate relation with the iterated homogenization theory proposed in this paper. In particular, we show that when specialized to the case of isotropic solids that contain an isotropic distribution of vacuous defects and that are subjected to hydrostatic loading (as worked out in Section 4.3), the total elastic energy (43)–(44) and current volume fraction of cavities (45)–(46) constructed via the

¹⁰ The critical pressure (86)₂ corresponds both to first Piola–Kirchhoff and to Cauchy pressure, since they are identical in this case because $\bar{\mathbf{F}}_{cr} = \bar{\lambda}_{cr} \mathbf{I} = \mathbf{I}$.

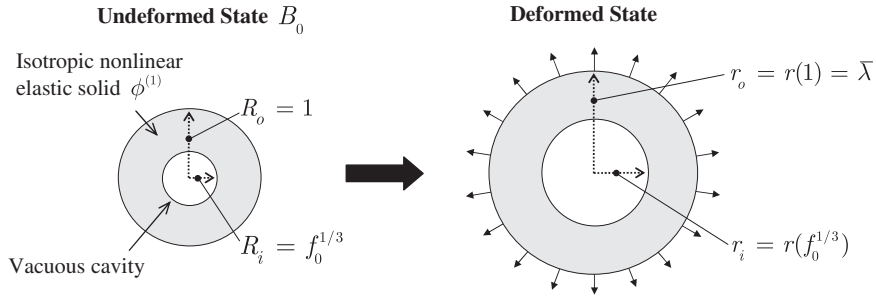


Fig. 4. Schematic illustrating the radially symmetric deformation of a unit spherical shell under external hydrostatic loading. The shell material is made up of an isotropic nonlinear elastic solid with stored-energy function $\phi^{(1)}$, while the cavity is vacuous. In its undeformed state, the shell has outer radius $R_o=1$ and inner radius $R_i=f_0^{1/3}$, with the prescribed quantity f_0 denoting the initial volume fraction of cavity (i.e., $f_0=R_i^3/R_o^3$). Upon loading, the spherical shell deforms into another spherical shell with outer radius $r_o=\bar{\lambda}$ and inner radius $r_i=r(f_0^{1/3})$, so that the volume fraction of cavity in the deformed shell is given by $f_B=r_i^3/r_o^3=r(f_0^{1/3})^3/\bar{\lambda}^3$.

iterated homogenization method of Section 3 reduce identically to the total elastic energy and current cavity volume fraction of a corresponding (i.e., with the same local constitutive behavior and initial cavity volume fraction) spherical shell undergoing radially symmetric deformations. The foremost implication of this connection is that the onset-of-cavitation criterion (48)–(50) proposed in this work can be thought of as a direct generalization of the classical criterion for radially symmetric cavitation to non-symmetric loading conditions, compressible anisotropic nonlinear elastic materials, and fairly general types of defects.

5.1. Radially symmetric response of a spherical shell under external hydrostatic loading

Consider a spherical shell with undeformed geometry defined by

$$B_0 = \{\mathbf{X} : f_0^{1/3} \leq |\mathbf{X}| \leq 1\} \tag{87}$$

that is made up of a homogeneous isotropic nonlinear elastic material with stored-energy function (76). Consider further that the shell is restricted to undergo radially symmetric deformations, for which \mathbf{x} has the form

$$\mathbf{x} = \frac{r(R)}{R} \mathbf{X}, \tag{88}$$

where $R=|\mathbf{X}|$, and that it is subjected to the boundary conditions

$$r(1) = \bar{\lambda} \quad \text{and} \quad \phi_1^{(1)}\left(r'(f_0^{1/3}), \frac{r(f_0^{1/3})}{f_0^{1/3}}, \frac{r(f_0^{1/3})}{f_0^{1/3}}\right) = 0, \tag{89}$$

where $\bar{\lambda}$ is the same positive loading parameter defined in (75) and the notation $r' = dr/dR$ has been utilized for convenience. The first of these boundary conditions states that the outer surface of the shell (i.e., $R=1$) is subjected to hydrostatic deformation, while the second condition states that the inner surface (i.e., $R=f_0^{1/3}$) is stress free, or in other words, that the cavity in the shell is vacuous, which is equivalent to condition (77)₂ above. Fig. 4 depicts schematically the above-posed boundary-value problem.

The equations of equilibrium associated with the above shell problem can be shown to reduce (see, e.g., Sivaloganathan, 1986) to the following nonlinear ordinary differential equation (ode):

$$\frac{d}{dR} \left[R^2 \phi_1^{(1)}\left(r', \frac{r}{R}, \frac{r}{R}\right) \right] = 2R \phi_2^{(1)}\left(r', \frac{r}{R}, \frac{r}{R}\right) \tag{90}$$

for the function r . For later reference, we also record that the equilibrium ode (90) can be written (see, e.g., Ball, 1982, Section 6) in the alternative form

$$\frac{d}{dR} \left\{ R^3 \left[\phi^{(1)}\left(r', \frac{r}{R}, \frac{r}{R}\right) - \left[r' - \frac{r}{R} \right] \phi_1^{(1)}\left(r', \frac{r}{R}, \frac{r}{R}\right) \right] \right\} = 3R^2 \phi^{(1)}\left(r', \frac{r}{R}, \frac{r}{R}\right). \tag{91}$$

In addition, the total elastic energy and current volume fraction of the cavity associated with the shell are given, respectively, by

$$E_B(\bar{\lambda}, f_0) = 3 \int_{f_0^{1/3}}^1 \phi^{(1)}\left(r', \frac{r}{R}, \frac{r}{R}\right) R^2 dR \tag{92}$$

and

$$f_B(\bar{\lambda}, f_0) = \left[\frac{r(f_0^{1/3})}{r(1)} \right]^3 = \frac{r^3(f_0^{1/3})}{\bar{\lambda}^3}, \tag{93}$$

where it is emphasized that the function r in these last two expressions corresponds to the solution of the ode (90) subject to the boundary conditions (89). Note, consequently, that r in (92) and (93) depends not only on R but also on the boundary data $\bar{\lambda}$ and f_0 , that is, in actuality, $r = r(R; \bar{\lambda}, f_0)$. In the sequel, for notational simplicity, we will utilize the notation $r(R)$ instead of $r(R; \bar{\lambda}, f_0)$ with the understanding that $r(R)$ is also a function of $\bar{\lambda}$ and f_0 . In passing, it is fitting to remark that the existence and uniqueness of solutions to the ode (90) have been studied by a number of researches, including Sivaloganathan (1986).

With the objective of establishing how the shell results (92) and (93) are related to the iterated homogenization results (79) and (81) of Section 4.3, we next rewrite (92) and (93) in a form that does not depend explicitly on the local field $r(R)$. We start by integrating the equilibrium equation (91) and then use the definition of total elastic energy (92) and the boundary conditions (89) to reach the following identity:

$$E_B(\bar{\lambda}, f_0) = \phi^{(1)}(r'(1), \bar{\lambda}, \bar{\lambda}) - [r'(1) - \bar{\lambda}] \phi_1^{(1)}(r'(1), \bar{\lambda}, \bar{\lambda}) - f_0 \phi^{(1)}\left(r'(f_0^{1/3}), \frac{r(f_0^{1/3})}{f_0^{1/3}}, \frac{r(f_0^{1/3})}{f_0^{1/3}}\right). \quad (94)$$

By making direct use of the definition (92), together with help of the equilibrium equation (90) and boundary conditions (89), it is also easy to show that

$$\begin{aligned} \frac{\partial E_B}{\partial \bar{\lambda}}(\bar{\lambda}, f_0) &= 3 \int_{f_0^{1/3}}^1 \frac{d}{dR} \left[R^2 \phi_1^{(1)}\left(r', \frac{r}{R}, \frac{r}{R}\right) \frac{\partial r}{\partial \bar{\lambda}} \right] dR \\ &= 3 \phi_1^{(1)}(r'(1), \bar{\lambda}, \bar{\lambda}), \\ \frac{\partial E_B}{\partial f_0}(\bar{\lambda}, f_0) &= -\phi^{(1)}\left(r'(f_0^{1/3}), \frac{r(f_0^{1/3})}{f_0^{1/3}}, \frac{r(f_0^{1/3})}{f_0^{1/3}}\right) + 3 \int_{f_0^{1/3}}^1 \frac{d}{dR} \left[R^2 \phi_1^{(1)}\left(r', \frac{r}{R}, \frac{r}{R}\right) \frac{\partial r}{\partial f_0} \right] dR \\ &= -\phi^{(1)}\left(r'(f_0^{1/3}), \frac{r(f_0^{1/3})}{f_0^{1/3}}, \frac{r(f_0^{1/3})}{f_0^{1/3}}\right). \end{aligned} \quad (95)$$

Now, differentiating expression (94) with respect to $\bar{\lambda}$ and equating the result to expression (95)₁ (i.e., setting $\partial E_B / \partial \bar{\lambda} = \partial E_B / \partial \bar{\lambda}$) leads to the following identity:

$$[r'(1) - \bar{\lambda}] \phi_{11}^{(1)}(r'(1), \bar{\lambda}, \bar{\lambda}) \frac{\partial}{\partial f_0} [r'(1)] = -2 f_0 \phi_2^{(1)}\left(r'(f_0^{1/3}), \frac{r(f_0^{1/3})}{f_0^{1/3}}, \frac{r(f_0^{1/3})}{f_0^{1/3}}\right) \frac{\partial}{\partial f_0} \left[\frac{r(f_0^{1/3})}{f_0^{1/3}} \right], \quad (96)$$

while differentiating expression (95)₁ with respect to f_0 , expression (95)₂ with respect to $\bar{\lambda}$, and equating the results (i.e., setting $\partial^2 E_B / \partial f_0 \partial \bar{\lambda} = \partial^2 E_B / \partial \bar{\lambda} \partial f_0$) leads to

$$3 \phi_{11}^{(1)}(r'(1), \bar{\lambda}, \bar{\lambda}) \frac{\partial}{\partial f_0} [r'(1)] = -2 \phi_2^{(1)}\left(r'(f_0^{1/3}), \frac{r(f_0^{1/3})}{f_0^{1/3}}, \frac{r(f_0^{1/3})}{f_0^{1/3}}\right) \frac{\partial}{\partial \bar{\lambda}} \left[\frac{r(f_0^{1/3})}{f_0^{1/3}} \right], \quad (97)$$

which, upon combining with (96), finally renders the ode

$$-f_0 \frac{\partial}{\partial f_0} \left[\frac{r(f_0^{1/3})}{f_0^{1/3}} \right] + \frac{r'(1) - \bar{\lambda}}{3} \frac{\partial}{\partial \bar{\lambda}} \left[\frac{r(f_0^{1/3})}{f_0^{1/3}} \right] = 0 \quad (98)$$

for the radius of the cavity of the shell in the deformed configuration, as characterized by the quantity $r(f_0^{1/3})$.

Having determined relations (94)–(95), it is straightforward to deduce that the total elastic energy (92) of the shell satisfies the following initial-value problem:

$$f_0 \frac{\partial E_B}{\partial f_0} - E_B - \frac{r'(1) - \bar{\lambda}}{3} \frac{\partial E_B}{\partial \bar{\lambda}} + \phi^{(1)}(r'(1), \bar{\lambda}, \bar{\lambda}) = 0, \quad E_B(\bar{\lambda}, 1) = 0, \quad (99)$$

where the quantity $r'(1)$, which is ultimately a function of the applied macroscopic stretch $\bar{\lambda}$ and initial volume fraction of the cavity f_0 , is solution to the nonlinear algebraic equation

$$\phi_1^{(1)}(r'(1), \bar{\lambda}, \bar{\lambda}) = \frac{1}{3} \frac{\partial E_B}{\partial \bar{\lambda}}. \quad (100)$$

Furthermore, in view of relation (98), it is a simple matter to deduce that the current volume fraction of cavity (93) in the shell satisfies the initial-value problem

$$f_0 \frac{\partial f_B}{\partial f_0} - \left(1 + \frac{r'(1) - \bar{\lambda}}{\bar{\lambda}} \right) f_B - \frac{r'(1) - \bar{\lambda}}{3} \frac{\partial f_B}{\partial \bar{\lambda}} = 0, \quad f_B(\bar{\lambda}, 1) = 1, \quad (101)$$

where, again, the quantity $r'(1)$ is defined by expression (100). Here, it is worth emphasizing that while the pdes (99) and (101) are amenable to numerical solutions — perhaps even more so than the standard ode (90) together with (92) and (93) — it is in general not possible to solve them in explicit form. For the special case of incompressible materials, however, the constraint of incompressibility $C(\mathbf{F}) = \det \mathbf{F}(\mathbf{X}) - 1 = r^2 r' / R^2 - 1 = 0$ for $\mathbf{X} \in B_0$ implies that the radial

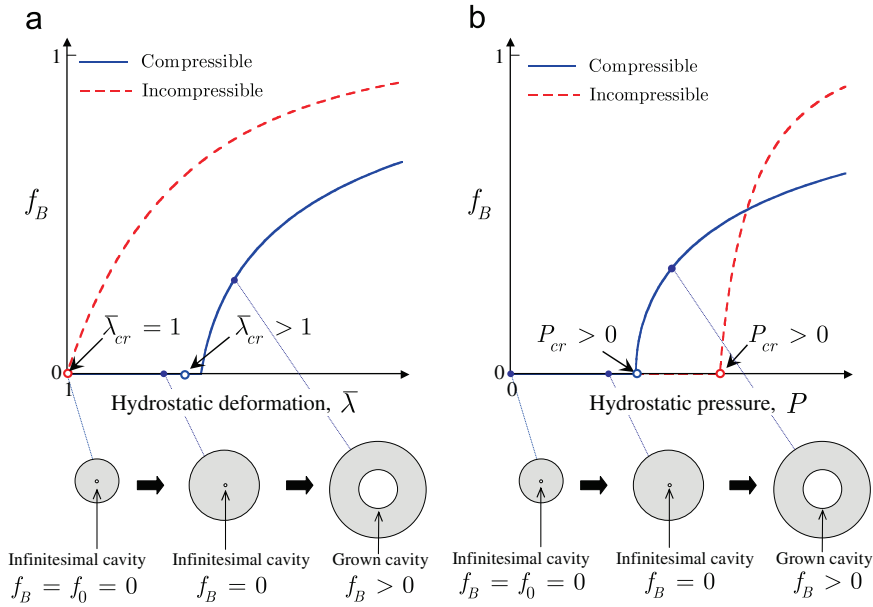


Fig. 5. Typical diagram illustrating the phenomenon of radially symmetric cavitation for compressible (solid line) and incompressible (dashed line) isotropic materials. The results show the evolution of the volume fraction of cavity, f_B , in a unit spherical shell with initially infinitesimal cavity ($f_0 \rightarrow 0+$) that is subjected to external hydrostatic loading. Part (a) shows f_B versus the applied deformation $\bar{\lambda}$, while part (b) shows f_B versus the resulting external hydrostatic pressure $P = (1/3)\partial E_B/\partial \bar{\lambda}$.

deformation of the shell must be of the form

$$r(R) = (R^3 + \bar{\lambda}^3 - 1)^{1/3}, \tag{102}$$

irrespectively of the specific choice of incompressible stored-energy function $\phi^{(1)}$. In view of (102), it is straightforward to solve the pdes (99) and (101) explicitly. Indeed, upon direct use of (102) and a little manipulation we obtain that the solutions read, respectively, as follows:

$$E_B(\bar{\lambda}, f_0) = 3(\bar{\lambda}^3 - 1) \int_{\bar{\lambda}}^{(1 + (\bar{\lambda}^3 - 1)/f_0)^{1/3}} \frac{z^2}{(z^3 - 1)^2} \phi^{(1)}(z^{-2}, z, z) dz \tag{103}$$

and

$$f_B(\bar{\lambda}, f_0) = \frac{\bar{\lambda}^3 - 1}{\bar{\lambda}^3} + \frac{f_0}{\bar{\lambda}^3}. \tag{104}$$

5.2. The criterion (48)–(50) as a generalization of the classical result for radially symmetric cavitation

The results presented in the preceding subsection are valid for shells with any value of initial volume fraction of cavity in the physical range $f_0 \in [0, 1]$. Their limiting behavior as $f_0 \rightarrow 0+$, when the shell cavity reduces to a zero-volume vacuous spherical cavity or *point defect*, lead to the classical result for radially symmetric cavitation of isotropic nonlinear elastic solids (Ball, 1982; Sivaloganathan, 1986). This limiting behavior is illustrated in Fig. 5. Part (a) shows typical results — for both compressible (solid line) and incompressible (dashed line) materials — for the current volume fraction of cavity f_B in the limit as $f_0 \rightarrow 0+$, as a function of the applied deformation $\bar{\lambda}$. Part (b) shows corresponding results for f_B , as a function of the resulting external pressure $P = (1/3)\partial E_B/\partial \bar{\lambda}$.¹¹

At this point, a quick glance suffices to recognize that by setting $r'(1) = \bar{\lambda} + \omega$ equations (99)–(101) are actually identical to equations (79)–(81) for any applied load $\bar{\lambda}$ and initial cavity size f_0 . That is, when specialized to the case of isotropic solids (76) that contain an isotropic distribution of vacuous defects (77) and that are subjected to hydrostatic loading (75),

¹¹ For the case of compressible materials, f_B is infinitesimal in the undeformed ($\bar{\lambda} = 1$) stress-free ($P = 0$) configuration and remains infinitesimally small for large deformations $\bar{\lambda} > 1$ until a critical deformation $\bar{\lambda}_{cr} > 1$, with associated critical pressure $P_{cr} > 0$, is reached at which it abruptly becomes finite, signaling the onset of cavitation. In general, the values of $\bar{\lambda}_{cr}$ and P_{cr} must be computed numerically, since Eqs. (99) and (101) do not admit explicit solutions for most compressible stored-energy functions $\phi^{(1)}$. For the simpler case of incompressible materials, it immediately follows from the explicit solutions (103) and (104) that $\bar{\lambda}_{cr} = 1$ and $P_{cr} = \int_1^\infty (1/(z^3 - 1))(d\phi^{(1)}/dz)(z^{-2}, z, z) dz$.

the total elastic energy (43)–(44) and current volume fraction of cavities (45)–(46) constructed via the iterated homogenization method of Section 3 *agree identically* with the total elastic energy and current cavity volume fraction of a corresponding spherical shell undergoing radially symmetric deformations. This is a remarkable connection given that the distribution of cavities (i.e., the microstructure) in the “porous” solid constructed by the iterated homogenization procedure is quite different from the single spherical cavity (i.e., the microstructure) in the shell. There are, however, two similarities between these two material systems that might help explain their identical responses under hydrostatic loading: (i) the deformation in the cavities in the formulation (43)–(46), as proved in Appendix C, is *uniform*, exactly as the deformation in the cavity of a radially deformed spherical shell, and (ii) the distribution of cavities in the formulation (43)–(46) is somewhat similar to the distribution of cavities in a hollow-sphere assemblage of Hashin (1985), whose response under hydrostatic loading happens to be identical to that of just a corresponding single spherical shell undergoing radially symmetric deformations.

In view of the above-revealed connection between the homogenization formulation (43)–(46) and the response of spherical shells for any value of f_0 — including the limiting case of $f_0 \rightarrow 0+$ — it follows that the onset-of-cavitation criterion (48)–(50) proposed in this work recovers Ball’s classical result for the critical load at which radially symmetric cavitation ensues in an isotropic (compressible as well as incompressible) material under hydrostatic loading. The criterion (48)–(50) can thus be thought of as an extension of the classical result to deal with arbitrary 3D loading conditions, compressible anisotropic materials, and random distributions of nonlinear elastic defects.

6. Concluding remarks

In deriving the cavitation criterion of Section 4 we have considered a representative material volume of sufficiently large size so that the distribution of defects within it is statistically uniform. In practice, the size of a macroscopic specimen is typically much larger than the size of such a representative volume so that a *two-scale* interpretation can be adopted. This is shown schematically in Fig. 6. On a microscopic scale the material consists of a continuous matrix containing a random distribution of defects, while on a macroscopic scale the material can be regarded as homogeneous.¹² From a macroscopic standpoint, the criterion then states that at any given material point of a specimen cavitation occurs whenever the deformation gradient at that point first satisfies conditions (48)–(50).

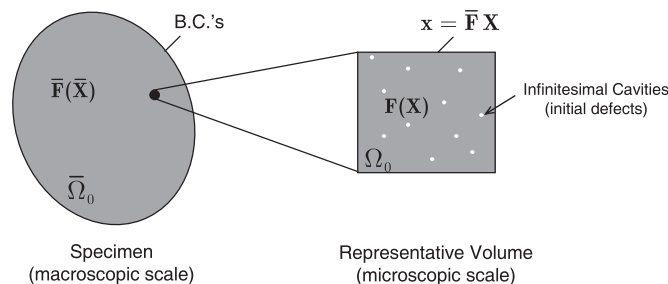


Fig. 6. Schematic of the two-scale interpretation. On a microscopic scale the material consists of a continuous matrix containing a statistically uniform distribution of defects, while on a macroscopic scale the material can be regarded as homogeneous. At any given material point $\bar{\mathbf{X}}$ in the specimen cavitation occurs whenever the macroscopic deformation $\bar{\mathbf{F}}(\bar{\mathbf{X}})$ at that point satisfies the criterion (48)–(50), where the functions f_i and $\bar{\mathbf{S}}$ depend on the solution of the elastostatics problem in the underlying representative volume.

As a first application, the theory developed in this work is utilized in the companion paper Lopez-Pamies et al. (in press) to derive an explicit onset-of-cavitation criterion for Neo-Hookean solids, containing a random isotropic distribution of vacuous defects, under general 3D loading conditions. Further applications of the theory to thoroughly investigate the effects of material compressibility and anisotropy, geometrical and mechanical features of the underlying defects, and loading conditions on when and how cavitation ensues in elastomeric solids will be presented in future works.

Within an actual elastomeric solid, the growth of a cavitating defect is expected to eventually lead to the fracture of the underlying polymer chains surrounding the defect (Gent, 1991). It would be interesting to extend our results to account for this transition from cavitation to fracture; the work of Williams and Schapery (1965) would be helpful here. It would also be worth exploiting the ideas presented in this work to study cavitation in other classes of materials — such as metals (Puttick, 1959; Ashby et al., 1989; Hou and Abeyaratne, 1992) and solids with growth (Pence and Tsai, 2007; Kundu and Crosby, 2009; McMahon and Goriely, 2010; Goriely et al., 2010; Cai et al., 2010) — where the occurrence of cavitation

¹² The macroscopic material response is given by the homogenized response function (49)₂. In general, this function will depend on the properties of the underlying defects even if their volume fraction is vanishingly small. In many cases of practical interest, however, the homogenized response function is expected to agree exactly with that of the defect-free solid before the onset of cavitation. This is for instance the case of the application considered in the companion paper (Lopez-Pamies et al., in press).

instabilities, much like in elastomeric solids, can also lead to material failure or be used to an advantage (Lopez-Pamies, 2010b).

Acknowledgments

Support for this work by the National Science Foundation (USA) through Grants DMS-1009503 and CMMI-1055528 is gratefully acknowledged. M.I.I. would also like to acknowledge support from CONICET (Argentina) under Grant PIP 00394/10.

Appendix A. Derivation of Eq. (45) for the current volume fraction of cavities f

In this appendix, we sketch out the derivation of Eq. (45) for the current volume fraction of cavities f . We begin by recognizing from the definition (12) that the computation of f amounts to the computation of the volume average of the determinant of the deformation-gradient field in the cavities $1/|\Omega_0^{(2)}| \int_{\Omega_0^{(2)}} \det \mathbf{F} \, d\mathbf{X}$, which is nothing more than certain trace of the third moment $1/|\Omega_0^{(2)}| \int_{\Omega_0^{(2)}} \mathbf{F} \otimes \mathbf{F} \otimes \mathbf{F} \, d\mathbf{X}$. In this connection, we recall that deformation field statistics in heterogeneous materials can be expediently computed from the total elastic energies of suitably perturbed problems (see, e.g., Idiart and Ponte Castañeda, 2006 and references therein). Specifically, for the case of interest here it is not difficult to deduce that

$$\bar{J}^{(2)} \doteq \frac{1}{|\Omega_0^{(2)}|} \int_{\Omega_0^{(2)}} \det \mathbf{F} \, d\mathbf{X} = 1 + \frac{1}{f_0} \left. \frac{\partial E_\tau}{\partial \tau} \right|_{\tau=0}, \quad (105)$$

where

$$E_\tau = \min_{\mathbf{F} \in \mathcal{K}^+(\bar{\mathbf{F}})} \frac{1}{|\Omega_0|} \int_{\Omega_0} [(1-\theta_0(\mathbf{X}))W^{(1)}(\mathbf{F}) + \theta_0(\mathbf{X})W_\tau^{(2)}(\mathbf{F})] \, d\mathbf{X} \quad (106)$$

and

$$W_\tau^{(2)}(\mathbf{F}) = W^{(2)}(\mathbf{F}) + \tau(\det \mathbf{F} - 1). \quad (107)$$

In the above relations, E_τ is the total elastic energy of a material system with cavities as defined in Section 2, but with perturbed stored-energy function for the cavities of the form (107). The scalar τ is a perturbation (material) parameter, such that for $\tau = 0$ the perturbed energy $W_\tau^{(2)}$ reduces to the original energy $W^{(2)}$.

For the class of material systems considered in Section 3, the function E_τ is solution to the Hamilton–Jacobi equation

$$f_0 \frac{\partial E_\tau}{\partial f_0} - E_\tau - \max_{\boldsymbol{\omega}(\boldsymbol{\xi})} \left\langle \boldsymbol{\omega} \cdot \frac{\partial E_\tau}{\partial \bar{\mathbf{F}}} \boldsymbol{\xi} - W^{(1)}(\bar{\mathbf{F}} + \boldsymbol{\omega} \otimes \boldsymbol{\xi}) \right\rangle = 0 \quad (108)$$

with initial condition given by

$$E_\tau(\bar{\mathbf{F}}, 1) = W_\tau^{(2)}(\mathbf{F}). \quad (109)$$

By differentiating Eq. (108) throughout with respect to τ , we obtain (in indicial notation)

$$f_0 \frac{\partial}{\partial f_0} \left(\frac{\partial E_\tau}{\partial \tau} \right) - \frac{\partial E_\tau}{\partial \tau} - \left\langle \omega_k \frac{\partial}{\partial \bar{F}_{kl}} \left(\frac{\partial E_\tau}{\partial \tau} \right) \xi_l \right\rangle = 0, \quad (110)$$

where $\boldsymbol{\omega}$ is the maximizing vector in (108). Making use of the identity (105) for the case of $\tau = 0$ in this expression yields the following equation for the average determinant $\bar{J}^{(2)}(\bar{\mathbf{F}}, f_0)$:

$$f_0 \frac{\partial \bar{J}^{(2)}}{\partial f_0} - \frac{\partial \bar{J}^{(2)}}{\partial \bar{F}_{kl}} \langle \omega_k \xi_l \rangle = 0 \quad (111)$$

subject to the initial condition

$$\bar{J}^{(2)}(\bar{\mathbf{F}}, 1) = \det \bar{\mathbf{F}}, \quad (112)$$

where now, since $\tau = 0$, $\boldsymbol{\omega}$ is nothing more than the maximizing vector in (43). Making in turn the use of the definition (12) in Eq. (111), finally leads to the following linear first-order pde for the current volume fraction of cavities $f(\bar{\mathbf{F}}, f_0)$:

$$f_0 \frac{\partial f}{\partial f_0} - (1 + \bar{\mathbf{F}}^{-T} \cdot \langle \boldsymbol{\omega} \otimes \boldsymbol{\xi} \rangle) f - \frac{\partial f}{\partial \bar{\mathbf{F}}} \cdot \langle \boldsymbol{\omega} \otimes \boldsymbol{\xi} \rangle = 0 \quad (113)$$

subject to the initial condition

$$f(\bar{\mathbf{F}}, 1) = 1. \quad (114)$$

Appendix B. The relation between $v(\xi)$ and the two-point probability $p^{(22)}$

The weighting function $v(\xi)$ in the orientational average (40) is shown here to be directly related to the two-point probability (5). The proof makes use of the well-known exact result for weakly inhomogeneous two-phase composites in the linearly elastic regime as $\bar{\mathbf{F}} \rightarrow \mathbf{I}$ (Willis, 1981, 1982; Milton, 2002, Chapter 15). In this regime, the effective stored-energy function of any two-phase composite with local energies (2) admits an expansion of the form

$$E = \frac{1}{2} \bar{\boldsymbol{\varepsilon}} \cdot \hat{\mathcal{L}} \bar{\boldsymbol{\varepsilon}} + O(\|\bar{\mathbf{F}} - \mathbf{I}\|^3), \quad (115)$$

where $\bar{\boldsymbol{\varepsilon}} = (\bar{\mathbf{F}} + \bar{\mathbf{F}}^T - 2\mathbf{I})/2$ is the macroscopic infinitesimal strain tensor and $\hat{\mathcal{L}} = \partial^2 E(\mathbf{I})/\partial \bar{\mathbf{F}}^2$ is the effective modulus tensor of the composite. When the heterogeneity contrast between the local modulus tensors $\Delta \mathcal{L} \doteq \mathcal{L}^{(2)} - \mathcal{L}^{(1)}$ is small, the tensor $\hat{\mathcal{L}}$ is given by

$$\hat{\mathcal{L}} = c_0^{(1)} \mathcal{L}^{(1)} + c_0^{(2)} \mathcal{L}^{(2)} - c_0^{(1)} c_0^{(2)} \Delta \mathcal{L} \mathcal{P}^{(1)} \Delta \mathcal{L} + O(\|\Delta \mathcal{L}\|^3), \quad (116)$$

where $c_0^{(1)}$ and $c_0^{(2)}$ denote the volume fractions of phases 1 and 2, respectively, and $\mathcal{P}^{(1)}$ is a microstructural fourth-order tensor given by

$$\mathcal{P}^{(1)} = -\frac{1}{8\pi^2} \int_{|\xi|=1} \mathcal{H}^{(1)}(\xi) \frac{\partial^2 h^*}{\partial p^2}(p, \xi) \Big|_{p=0} d\xi. \quad (117)$$

In this expression,

$$\mathcal{H}_{ijkl}^{(1)}(\xi) = [K_{ik}^{(1)}(\xi)]^{-1} \xi_j \xi_l, \quad K_{ik}^{(1)}(\xi) = \mathcal{L}_{ijkl}^{(1)} \xi_j \xi_l, \quad h^*(p, \xi) = \int_{\mathbb{R}^3} h(\mathbf{X}) \delta(\xi \cdot \mathbf{X} - p) d\mathbf{X}, \quad (118)$$

where $\mathbf{K}^{(1)}$ denotes the so-called acoustic tensor of the matrix material, and $h^*(p, \xi)$ is the Radon transform of the two-point correlation function $h(\mathbf{X})$ defined in (5). Thus, to second order in deformation and in heterogeneity contrast, the exact total elastic energy (115) depends on the angular variation — but not on the radial variation — of the two-point probability through the tensor $\mathcal{P}^{(1)}$.

Given that the result (43)–(44) is exact for a certain class of composites, it should reduce to the exact result (115) for weakly inhomogeneous composites in the linearly elastic regime. Therefore, the solution E to the Hamilton–Jacobi equation (43) in the linearly elastic regime must be of the form

$$E(\bar{\mathbf{F}}, f_0) = \frac{1}{2} \bar{\boldsymbol{\varepsilon}} \cdot \hat{\mathbf{L}}(f_0) \bar{\boldsymbol{\varepsilon}} + O(\|\bar{\mathbf{F}} - \mathbf{I}\|^3), \quad (119)$$

where $\hat{\mathbf{L}}(f_0) = \partial^2 E(\mathbf{I}, f_0)/\partial \bar{\mathbf{F}}^2$ is a tensor of elastic moduli. To find $\hat{\mathbf{L}}(f_0)$, we first expand the optimality condition in (43) to first order in the deformation, making use of (119), to get

$$\boldsymbol{\omega} \otimes \boldsymbol{\xi} = \mathcal{H}^{(1)}(\boldsymbol{\xi}) \Delta \hat{\mathbf{L}} \bar{\boldsymbol{\varepsilon}} + O(\|\bar{\mathbf{F}} - \mathbf{I}\|^2), \quad (120)$$

where $\Delta \hat{\mathbf{L}} \doteq \hat{\mathbf{L}} - \mathcal{L}^{(1)}$ and $\mathcal{H}^{(1)}(\boldsymbol{\xi})$ has been defined in (118)₁. Then, introducing (120) into the Hamilton–Jacobi equation (43) and expanding to order $\|\bar{\mathbf{F}} - \mathbf{I}\|^2$ we obtain the following Riccati equation for $\hat{\mathbf{L}}(f_0)$:

$$f_0 \frac{\partial \hat{\mathbf{L}}}{\partial f_0} - \Delta \hat{\mathbf{L}} - \Delta \hat{\mathbf{L}} \mathcal{P}^{(1)} \Delta \hat{\mathbf{L}} = \mathbf{0}, \quad \hat{\mathbf{L}}(1) = \mathcal{L}^{(2)}, \quad (121)$$

where

$$\mathbf{P}^{(1)} = \int_{|\xi|=1} \mathcal{H}^{(1)}(\xi) v(\xi) d\xi \quad (122)$$

is a microstructural tensor containing the distributional function $v(\xi)$. The solution to Eq. (121) is

$$\hat{\mathbf{L}} = \mathcal{L}^{(1)} + f_0 [(1 - f_0) \mathbf{P}^{(1)} + (\Delta \mathcal{L})^{-1}]^{-1}. \quad (123)$$

Finally, expanding this result to second order in the contrast $\|\Delta \mathcal{L}\|$ we get an expression of the same form (116) but with the tensor $\mathcal{P}^{(1)}$ replaced by $\mathbf{P}^{(1)}$ and $c_0^{(1)}$ and $c_0^{(2)}$ replaced by $1 - f_0$ and f_0 . By comparing (117) and (122) we conclude that the two expansions match provided

$$v(\xi) = -\frac{1}{8\pi^2} \frac{\partial^2 h^*}{\partial p^2}(p, \xi) \Big|_{p=0}, \quad (124)$$

where h^* is the Radon transform of the two-point correlation function h as defined in (118)₃. This is the relation between the weighting function $v(\xi)$ and the two-point probability (5).

As pointed out in the main body of the text, the two-point probability contains information about the shape and spatial distribution of the cavities; the interested reader is referred to the works Willis (1977) and Ponte Castañeda and Willis (1995) for an in-depth discussion of this issue. A case of particular relevance for applications is that of microstructural isotropy, corresponding for instance to spherical cavities whose centers are distributed with “spherical” symmetry. In this

case, $h(\mathbf{X}) = h_{iso}(|\mathbf{X}|)$ and the Radon transform (118)₃ specializes to

$$h^*(p, \xi) = 2\pi \int_p^\infty h_{iso}(r)r \, dr \quad \text{and therefore} \quad \frac{\partial^2 h^*}{\partial p^2}(p, \xi) = -2\pi[p h'_{iso}(p) + h_{iso}(p)]. \quad (125)$$

In view of (124) and the fact that $h_{iso}(0) = 1$, we conclude that the function $v(\xi)$ for isotropic microstructures of cavities is simply given by

$$v(\xi) = \frac{1}{4\pi}. \quad (126)$$

Appendix C. Proof of the uniformity of the fields in the cavities in the formulation (43)–(46)

In order to prove that the deformation gradient field in the cavities, $\mathbf{F}(\mathbf{X})$ for $\mathbf{X} \in \Omega_0^{(2)}$, is uniform in the formulation (43)–(46), our strategy here is first to compute the average deformation gradient $\bar{\mathbf{F}}^{(2)} \doteq 1/|\Omega_0^{(2)}| \int_{\Omega_0^{(2)}} \mathbf{F} \, d\mathbf{X}$ and the second moment $\bar{\mathcal{C}}^{(2)} \doteq 1/|\Omega_0^{(2)}| \int_{\Omega_0^{(2)}} \mathbf{F} \otimes \mathbf{F} \, d\mathbf{X}$, and then show that these quantities satisfy the relation $\bar{\mathcal{C}}^{(2)} = \bar{\mathbf{F}}^{(2)} \otimes \bar{\mathbf{F}}^{(2)}$.

Thus, by making use of the perturbation technique discussed in Appendix A, it is straightforward to show that the average deformation gradient in the cavities $\bar{\mathbf{F}}^{(2)}$ is the solution to the initial-value problem

$$f_0 \frac{\partial \bar{\mathbf{F}}_{ij}^{(2)}}{\partial f_0} - \frac{\partial \bar{\mathbf{F}}_{ij}^{(2)}}{\partial \bar{\mathbf{F}}_{mn}} \langle \omega_m \xi_n \rangle = 0, \quad \bar{\mathbf{F}}_{ij}^{(2)}(\bar{\mathbf{F}}, 1) = \bar{\mathbf{F}}_{ij}, \quad (127)$$

and that the second moment $\bar{\mathcal{C}}^{(2)}$ is solution to

$$f_0 \frac{\partial \bar{\mathcal{C}}_{ijkl}^{(2)}}{\partial f_0} - \frac{\partial \bar{\mathcal{C}}_{ijkl}^{(2)}}{\partial \bar{\mathbf{F}}_{mn}} \langle \omega_m \xi_n \rangle = 0, \quad \bar{\mathcal{C}}_{ijkl}^{(2)}(\bar{\mathbf{F}}, 1) = \bar{\mathbf{F}}_{ij} \bar{\mathbf{F}}_{kl}. \quad (128)$$

In these expressions, again, ω is the maximizing vector in (43). Given (127) and (128), a quick calculation suffices to deduce that

$$\bar{\mathcal{C}}^{(2)} = \bar{\mathbf{F}}^{(2)} \otimes \bar{\mathbf{F}}^{(2)} \quad (129)$$

is a solution to (128) and hence that the deformation gradient field in the cavities is uniform. By the same token, the stress in the cavities is also uniform and simply given by $\bar{\mathbf{S}}^{(2)} \doteq 1/|\Omega_0^{(2)}| \int_{\Omega_0^{(2)}} \mathbf{S}(\mathbf{X}) \, d\mathbf{X} = \partial W^{(2)}(\bar{\mathbf{F}}^{(2)})/\partial \bar{\mathbf{F}}$.

In passing, it is fitting to remark that the *uniform* deformation gradient $\bar{\mathbf{F}}^{(2)}$, as characterized by the linear pde (127)₁ and initial condition (127)₂, serves to define the *shape* of the cavities in the deformed configuration. Thus, considering the limit of $f_0 \rightarrow 0+$ in Eq. (127) permits to examine the deformed shape of the underlying defects in the context of cavitation problems.

References

- Antman, S.S., Negrón-Marrero, P.V., 1987. The remarkable nature of radially symmetric equilibrium states of aleotropic nonlinearly elastic bodies. *J. Elast.* 18, 131–164.
- Arridge, R.G.C., Folkes, M.J., 1972. The mechanical properties of a ‘single crystal’ of SBS copolymer—a novel composite material. *J. Phys. D: Appl. Phys.* 5, 344–358.
- Ashby, M.F., Blunt, F.J., Bannister, M., 1989. Flow characteristics of highly constrained metal wires. *Acta Metall.* 37, 1847–1857.
- Avellaneda, M., 1987. Iterated homogenization, differential effective medium theory, and applications. *Commun. Pure Appl. Math.* XL, 527–554.
- Ball, J.M., 1982. Discontinuous equilibrium solutions and cavitation in nonlinear elasticity. *Philos. Trans. R. Soc. A* 306, 557–611.
- Bayraktar, E., Bessri, K., Bathias, C., 2008. Deformation behaviour of elastomeric matrix composites under static loading conditions. *Eng. Fract. Mech.* 75, 2695–2706.
- Bischoff, J.E., Arruda, E.M., Grosh, K., 2001. A new constitutive model for the compressibility of elastomers at finite deformations. *Rubber Chem. Technol.* 74, 541–559.
- Benton, S.H., 1977. The Hamilton–Jacobi Equation: a Global Approach. *Mathematics in Science and Engineering*, vol. 131. Academic Press.
- Bourdin, B., Khon, R.V., 2008. Optimization of structural topology in the high-porosity regime. *J. Mech. Phys. Solids* 56, 1043–1064.
- Bridgman, P.W., 1945. The compression of sixty-one solid substances to 25,000 kg/cm, determined by a new rapid method. *Proc. Am. Acad. Arts Sci.* 76, 9–24.
- Bruggeman, D.A.G., 1935. Berechnung verschiedener physikalischer Konstanten von heterogenen Substanzen. I. Dielektrizitätskonstanten und Leitfähigkeiten der Mischkörper aus isotropen Substanzen [Calculation of various physical constants in heterogeneous substances. I. Dielectric constants and conductivity of composites from isotropic substances]. *Ann. Phys.* 416, 636–664 (in German).
- Cai, S., Bertoldi, K., Wang, H., Suo, Z., 2010. Osmotic collapse of a void in an elastomer: breathing, buckling and creasing. *Soft Matter* 6, 5770–5777.
- Chang, Y.-W., Gent, A.N., Padovan, J., 1993. Expansion of a cavity in a rubber block under unequal stresses. *Int. J. Fract.* 60, 283–291.
- Cheng, C., Hiltner, A., Baer, E., 1995. Cooperative cavitation in rubber-toughened polycarbonate. *J. Mater. Sci.* 30, 587–595.
- Cho, K., Gent, A.N., Lam, P.S., 1987. Internal fracture in an elastomer containing a rigid inclusion. *J. Mater. Sci.* 22, 2899–2905.
- Creton, C., Hooker, J., 2001. Bulk and interfacial contributions to the debonding mechanisms of soft adhesives: extension to large strains. *Langmuir* 17, 4948–4954.
- Cristiano, A., Marcellan, A., Long, R., Hui, C.Y., Stolk, J., Creton, C., 2010. An experimental investigation of fracture by cavitation of model elastomeric networks. *J. Polym. Sci. Part B: Polym. Phys.* 48, 1409–1422.
- deBotton, G., 2005. Transversely isotropic sequentially laminated composites in finite elasticity. *J. Mech. Phys. Solids* 53, 1334–1361.
- deBotton, G., Shmuel, G., 2010. A new variational estimate for the effective response of hyperelastic composites. *J. Mech. Phys. Solids* 58, 466–483.

- Dorfmann, A., 2003. Stress softening of elastomers in hydrostatic tension. *Acta Mech.* 165, 117–137.
- Duva, J.M., 1984. A self-consistent analysis of the stiffening effect of rigid inclusions on a power-law material. *ASME J. Eng. Mater. Technol.* 106, 317–321.
- Eshelby, J.D., 1957. The determination of the elastic field of an ellipsoidal inclusion and related problems. *Proc. R. Soc. London A* 241, 376–396.
- Fond, C., 2001. Cavitation criterion for rubber materials: a review of void-growth models. *J. Polym. Sci. Part B* 39, 2081–2096.
- Gent, A.N., 1991. Cavitation in rubber: a cautionary tale. *Rubber Chem. Technol.* 63, G49–G53.
- Gent, A.N., Lindley, P.B., 1959. Internal rupture of bonded rubber cylinders in tension. *Proc. R. Soc. London A* 249, 195–205.
- Gent, A.N., Tompkins, D.A., 1969a. Nucleation and growth of gas bubbles in elastomers. *J. Appl. Phys.* 40, 2520–2525.
- Gent, A.N., Tompkins, D.A., 1969b. Surface energy effects for small holes or particles in elastomers. *J. Polym. Sci. Part A2* 7, 1483–1487.
- Gent, A.N., Park, B., 1984. Failure processes in elastomers at or near a rigid inclusion. *J. Mater. Sci.* 19, 1947–1956.
- Geymonat, G., Müller, S., Triantafyllidis, N., 1993. Homogenization of nonlinearly elastic materials, microscopic bifurcation and macroscopic loss of rank-one convexity. *Arch. Ration. Mech. Anal.* 122, 231–290.
- Goriely, A., Moulton, D.E., Vandiver, R., 2010. Elastic cavitation, tube hollowing, and differential growth in plants and biological tissues. *Eur. Phys. Lett.* 91, 18001.
- Hashin, Z., 1985. Large isotropic elastic deformation of composites and porous media. *Int. J. Solids Struct.* 21, 711–720.
- Henao, D., 2009. Cavitation, invertibility, and convergence of regularized minimizers in nonlinear elasticity. *J. Elast.* 94, 55–68.
- Henao, D., Mora-Corral, C., 2010. Invertibility and weak continuity of the determinant for the modelling of cavitation and fracture in nonlinear elasticity. *Arch. Ration. Mech. Anal.* 197, 619–655.
- Hill, R., 1972. On constitutive macrovariables for heterogeneous solids at finite strain. *Proc. R. Soc. London A* 326, 131–147.
- Horgan, C.O., Abeyaratne, R., 1986. A bifurcation problem for a compressible nonlinearly elastic medium: growth of a micro-void. *J. Elast.* 16, 189–200.
- Horgan, C.O., Polignone, D.A., 1995. Cavitation in nonlinearly elastic solids: a review. *Appl. Mech. Rev.* 48, 471–485.
- Hou, H.-S., Abeyaratne, R., 1992. Cavitation in elastic and elastic-plastic solids. *J. Mech. Phys. Solids* 40, 571–592.
- Idiart, M.I., 2008. Modeling the macroscopic behavior of two-phase nonlinear composites by infinite-rank laminates. *J. Mech. Phys. Solids* 56, 2599–2617.
- Idiart, M.I., Ponte Castañeda, P., 2006. Field statistics in nonlinear composites. I. Theory. *Proc. R. Soc. London A* 463, 183–202.
- James, R.D., Spector, S.J., 1991. The formation of filamentary voids in solids. *J. Mech. Phys. Solids* 39, 783–813.
- Kundu, S., Crosby, A.J., 2009. Cavitation and fracture behavior of polyacrylamide hydrogels. *Soft Matter* 5, 3963–3968.
- Lopez-Pamies, O., 2010a. An exact result for the macroscopic response of particle-reinforced Neo-Hookean solids. *J. Appl. Mech.* 77, 021016.
- Lopez-Pamies, O., iMechanica, Journal Club, May 2010b. < <http://imechanica.org/node/8131> >.
- Lopez-Pamies, O., 2009. Onset of cavitation in compressible, isotropic, hyperelastic solids. *J. Elast.* 94, 115–145.
- Lopez-Pamies, O., Nakamura, T., Idiart, M.I. Cavitation in elastomeric solids: II—onset-of-cavitation surfaces for Neo-Hookean materials. *J. Mech. Phys. Solids*, in press. doi:10.1016/j.jmps.2011.04.016.
- Lopez-Pamies, O., Ponte Castañeda, P., 2009. Microstructure evolution in hyperelastic laminates and implications for overall behavior and macroscopic stability. *Mech. Mater.* 41, 364–374.
- Lopez-Pamies, O., Ponte Castañeda, P., 2007. Homogenization-based constitutive models for porous elastomers and implications for macroscopic instabilities. I—analysis. *J. Mech. Phys. Solids* 55, 1677–1701.
- Lopez-Pamies, O., Ponte Castañeda, P., 2006. On the overall behavior microstructure evolution and macroscopic stability in reinforced rubbers at large deformations. I—theory. *J. Mech. Phys. Solids* 54, 807–830.
- McMahon, J., Goriely, A., 2010. Spontaneous cavitation in growing elastic membranes. *Math. Mech. Solids* 15, 57–77.
- Merodio, J., Saccomandi, G., 2006. Remarks on cavity formation in fiber-reinforced incompressible non-linearly elastic solids. *Eur. J. Mech. A/Solids* 25, 778–792.
- Michel, J.C., Lopez-Pamies, O., Ponte Castañeda, P., Triantafyllidis, N., 2007. Microscopic and macroscopic instabilities in finitely strained porous elastomers. *J. Mech. Phys. Solids* 55, 900–938.
- Michel, J.C., Lopez-Pamies, O., Ponte Castañeda, P., Triantafyllidis, N., 2010. Microscopic and macroscopic instabilities in finitely strained fiber-reinforced elastomers. *J. Mech. Phys. Solids* 58, 1776–1803.
- Milton, G., 2002. *The Theory of Composites*. Cambridge University Press, Cambridge, UK.
- Müller, S., 1987. Homogenization of nonconvex integral functionals and cellular elastic materials. *Arch. Ration. Mech. Anal.* 99, 189–212.
- Müller, S., Spector, S.J., 1995. An existence theory for nonlinear elasticity that allows for cavitation. *Arch. Ration. Mech. Anal.* 131, 1–66.
- Nestorovic, N., Triantafyllidis, N., 2004. Onset of failure in finitely strained layered composites subjected to combined normal and shear strain. *J. Mech. Phys. Solids* 52, 941–974.
- Norris, A.N., 1985. A differential scheme for the effective moduli of composites. *Mech. Mater.* 4, 1–16.
- Pence, T.J., Tsai, S.J., 2007. Bulk cavitation and the possibility of localized deformation due to surface layer swelling. *J. Elast.* 87, 161–185.
- Pericak-Spector, K.A., Spector, S.J., 1988. Nonuniqueness for hyperbolic systems: cavitation in nonlinear elastodynamics. *Arch. Ration. Mech. Anal.* 101, 293–317.
- Polyanin, A.D., Zaitsev, V.F., Moussiaux, A., 2002. *Handbook of First Order Partial Differential Equations*. Taylor & Francis.
- Ponte Castañeda, P., Willis, J.R., 1995. The effect of spatial distribution on the effective behavior of composite materials and cracked media. *J. Mech. Phys. Solids* 43, 1919–1951.
- Puttick, K.E., 1959. Ductile fracture in metals. *Philos. Mag.* 4, 964–969.
- Sivaloganathan, J., 1986. Uniqueness of regular and singular equilibria for spherically symmetric problems of nonlinear elasticity. *Arch. Ration. Mech. Anal.* 96, 97–136.
- Sivaloganathan, J., 1999. On cavitation and degenerate cavitation under internal hydrostatic pressure. *Proc. R. Soc. London A* 455, 3645–3664.
- Sivaloganathan, J., Spector, S.J., 2000. On the existence of minimizers with prescribed singular points in nonlinear elasticity. *J. Elast.* 59, 83–113.
- Sivaloganathan, J., Spector, S.J., 2002. A construction of infinitely many singular weak solutions to the equations of nonlinear elasticity. *Proc. R. Soc. Ed.* 132A, 985–992.
- Sivaloganathan, J., Spector, S.J., Tilakraj, V., 2006. The convergence of regularized minimizers for cavitation problems in nonlinear elasticity. *SIAM J. Appl. Math.* 66, 736–757.
- Sohoni, G.B., Mark, J.E., 1987. Anisotropic reinforcement in elastomers containing magnetic filler particles. *J. Appl. Polym. Sci.* 34, 2853–2859.
- Steenbrink, A.C., Van der Giessen, E., 1999. On cavitation, post-cavitation and yield in amorphous polymer-rubber blends. *J. Mech. Phys. Solids* 36, 732–765.
- Stuart, C.A., 1985. Radially symmetric cavitation for hyperelastic materials. *Ann. Inst. H. Poincaré Anal. Non linéaire* 2, 33–66.
- Warner, M., Terentjev, E.M., 2005. *Liquid Crystal Elastomers*. Oxford Science Publications.
- Williams, M.L., Schapery, R.A., 1965. Spherical flaw instability in hydrostatic tension. *Int. J. Fract. Mech.* 1, 64–72.
- Willis, J.R., 1977. Bounds and self-consistent estimates for the overall moduli of anisotropic composites. *J. Mech. Phys. Solids* 25, 185–202.
- Willis, J.R., 1981. Variational and related methods for the overall properties of composites. *Adv. Appl. Mech.* 21, 1–78.
- Willis, J.R., 1982. Elasticity theory of composites. In: Hopkins, H.G., Sewell, M.J. (Eds.), *Mechanics of Solids, The Rodney Hill 60th Anniversary Volume*. Pergamon Press, pp. 653–686.
- Xu, X., Henao, D. An efficient numerical method for cavitation in nonlinear elasticity. *Math. Models Methods Appl. Sci.*, in press, doi:10.1142/S0218202511005556.